231 (2023) 212405

Contents lists available at ScienceDirect

Geoenergy Science and Engineering

journal homepage: www.sciencedirect.com/journal/geoenergy-science-and-engineering

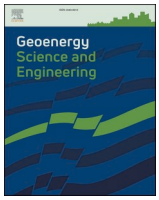

A mitigation strategy for productivity impairment in sandstone reservoirs with varying clay mineralogy

Michael Chuks Halim [a], Hossein Hamidi [a,*], Kirsty Houston [b]

[a] School of Engineering, King's College, University of Aberdeen, Aberdeen AB24 3UE, UK
[b] M.I. SWACO, A Schlumberger Company, Aberdeen, UK

ARTICLE INFO

Keywords:
Formation damage
Clay mineralogy
Reservoir rock
Optimizing productivity
Permeability impairment
Wellbore

ABSTRACT

The interaction between drilling fluids and oil and gas reservoir formations can result in the reduction or blockage of the micropore structural network, leading to a consequent decrease in permeability. Due to the negative economic impact of formation damage on hydrocarbon production, formulating drilling fluids with characteristics that minimise formation damage has been a major focus of the petroleum industry and researchers since the 1970s–1980s. Formation damage can significantly affect the ultimate productivity in hydrocarbon-bearing formations, especially in sandstone reservoirs with varying clay mineralogy such as kaolinite, smectite, illite, and mixed layer (illite + smectite) clay mineralogy in the micropore structural networks. These clay minerals are highly unstable/reactive and often appear as pore lining, pore bridging, and pore-filling along the walls of the micropore structural, inevitably coming into contact with drilling fluids (both solids and filtrates) that have invaded the micropore structure. Existing studies on the understanding of the relationship between drilling fluid formulation and formation damage mechanisms have not adequately addressed the role of individual species of clay minerals and their varying physicochemical properties during the formulation of drilling fluids for sandstone reservoirs with varying clay minerals. Instead, clay minerals are often treated as a whole or a single group. The work presented in this paper aims to examine and quantifies the impact of three drilling fluids (PAC-UL water-based, potassium formate, and halide drilling fluids) on productivity impairment in kaolinitic sandstone reservoirs and in kaolinitic and mixed-layer (illitic + smectitic) sandstone reservoirs. To achieve this, a high-temperature, high-pressure (HTHP) formation damage testing facility was designed and built to determine the initial and return permeability of selected hydrocarbon reservoirs using core samples. The formation damage mechanisms resulting from the interaction of the reservoir rocks with different formulations of drilling fluids are fully characterized using a combination of scanning electron microscopy, energy dispersive X-ray and micro-computed tomography. For all three drilling fluid formulations, the results showed an enhanced return permeability of the kaolinitic sandstone after interaction with the specially formulated halide drilling fluid.

1. Introduction

Despite significant achievements made in reducing the costs of renewable energy technologies and embracing their use, oil and gas account for more than 75% of overall energy utilized especially in developing countries around the world (Kibria et al., 2019) and 60% of global energy consumption (Filimonova et al., 2020). Furthermore, global total energy consumption is expected to rise at a growth rate of 1.5% per year in energy demand from 2015 to 2040 (International Energy Agency, 2020). Undisrupted supply and access to oil and gas, contributing to the energy mix in a net-zero economy, especially in addressing energy poverty would help equitably provide available, affordable, reliable, and efficient energy services to many end-users.

Oil and gas production involves drilling oil wells and extracting hydrocarbons with the aim of refining and subsequently selling the oil, gas, and associated refined products (Klepikov and Klepikov, 2020; Rui et al., 2018). It requires a significant capital investment and long lead times to find and extract the hydrocarbons, sometimes under challenging environmental conditions with substantial risks (Rui et al., 2018; Epelle and Gerogiorgis, 2020). To share the involved risk, exploration, development and production activities are sometimes carried out as joint ventures activities due to the substantial capital cost

* Corresponding author.
E-mail address: hossein.hamidi@abdn.ac.uk (H. Hamidi).

https://doi.org/10.1016/j.geoen.2023.212405
Received 21 June 2023; Received in revised form 26 September 2023; Accepted 11 October 2023
Available online 18 October 2023

(Rui et al., 2018). The natural resources of oil and gas found by major petroleum producing companies are their most important economic asset (Klepikov and Klepikov, 2020). The financial strength of the major petroleum producing companies lies in the total recovery factor or recoverability of the oil and gas reserves from the oil and gas-bearing formations or reservoirs (Rui et al., 2018; Epelle and Gerogiorgis, 2020).

One major cause of low recoverability of oil and gas from producing formation is the process known as formation damage (Monaghan et al., 1959; Zhao et al., 2018; Adebayo and Bageri, 2020). Formation damage is the process that reduces the natural inherent productivity of an oil or gas-producing formation or the injectivity of a water or gas injection well (Bennion, 2002; Fleming et al., 2020) due to blockage of the flow path. Formation damage is inevitable and can occur during drilling, completion, workover, stimulation, and production operations throughout the lifespan of a well (Bennion, 2002). Formation damage can occur due to various reasons, one of them being drilling fluids used during the drilling of horizontal or vertical wells, which is particularly prominent in barefooted sandstone reservoirs (Bennion, 2002; Masikewich and Bennion, 1999; Kang and Luo, 2007).

Understanding the physics and mechanics of fluid flow in porous media has been of great interest to the oil and gas industry and various academic disciplines, including petroleum engineering and geology, as formation damage inhibits the flow of fluids through porous formations. The characterization of the formation properties that affect fluid flow in porous media, particularly permeability, has found important applications in predicting pore throat size and distribution and the degree of change in the formation properties (Aminian et al., 1998). Knowledge of formation properties, especially permeability, is crucial to flow prediction within the interconnected pores of rocks (Muskat et al., 1937) because the plugging of the pores results in permeability reduction, known as formation damage (Aminian et al., 1998; Darley and Gray, 2011).

The intensity of permeability alteration or plugging of pores is influenced by the efficiency of drilling fluid, as an efficient drilling fluid will form an efficient filter cake that will minimizes drilling fluid filtrate invasion (Adebayo and Bageri, 2020). Drilling fluid's filtrate invasion during drilling operations is the primary source of formation damage (Adebayo and Bageri, 2020). Once production capacity is drastically reduced due to formation damage, the investment in exploration becomes worthless (Zhao et al., 2018). Therefore, economic failure during the development of these oil and gas fields may occur due to well abandonment or shortened field life, unless the physicochemical changes resulting from the interaction between drilling fluids and clay mineralogy, which cause permeability reduction, are properly understood. Shell estimated that the cost of formation damage on their operated assets was $1 billion per year, accounting for approximately 3.3% of the total world crude oil production at that time (Byrne, 2010). The ability to accurately predict and mitigate against formation damage is therefore critical to the oil and gas industry.

Due to the negative economic impact of formation damage on hydrocarbon production, the formulation of drilling fluids that minimise formation damage within the micropore structural networks was a major focus of the oil and gas industry and researchers in the 1970s and 1980s and it continues to be a major focus today. Correspondingly, the approach for formation damage mitigation or formation damage control (FDM/FDC) for micropore structural networks has become an important countermeasure in exploring, drilling, developing, and producing hydrocarbon from sandstone reservoirs (Kang et al., 2014, 2019). The FDM/FDC approach for micropore structural networks, including the use of specially formulated minimally damaging drilling fluids, could result in optimizing the productivity index of sandstone reservoirs (S Siddig et al., 2020).

Drilling fluids are mixtures of solid additives present as discontinuous phases spread within a liquid continuous phase (S Siddig et al., 2020). Drilling fluids are formulated and designed to achieve different operational objectives (S Siddig et al., 2020; Swaco, 2008). These objectives include cooling the drill bits and aiding in cleaning the holes of drilled wells by carrying drill cuttings to the surface while maintaining hole stability. Additionally, they prevent the invasion of formation fluids into the wellbores by creating a low permeability layer known as the filter cake on the walls of the wellbore (Swaco, 2008; Hossain and Al-Majed, 2015; Bourgoyne et al., 1986). The filter cake can also reduce the invasion of drilling fluids into the micropore structural networks of the drilled formation (Hossain and Al-Majed, 2015; Bourgoyne et al., 1986). This means that drilling fluids inevitably interact with these formations, including their fluids and solid clay mineralogy content, within the micropore structural networks. Therefore, achieving optimum well productivity with minimal formation damage to sandstone reservoirs and ensuring safe drilling and completion operations depends on the characteristics and composition of the drilling fluids (Karakosta et al., 2020) used in the FDM/FDC measure for micropore structural networks.

The key to effectively implementing the FDM/FDC measure for micropore structural networks of sandstone reservoirs lies in designing and formulating drilling fluid performance. This includes the optimizing particle size distribution (PSD), determining particle concentration, and designing drilling fluid rheological properties (Abrams, 1977; Smith et al., 1996; Suri and Sharma, 2004; Xu et al., 2018; Longeron et al., 2000; Jiaojiao et al., 2010; Bailey et al., 2000). Among these characteristics, designing (Francis et al., 1995) optimal solids' (PSD) is one of the key factors in minimising formation damage caused by the invasion of drilling fluids into micropore structural networks (Kang et al., 2019), as it is closely linked to the build-up of a thin impermeable layer called the filter cake on the wellbore surface (S Siddig et al., 2020; Engelhardt, 1954). Thin filter encrust with low permeability can effectively prevent the invasion of drilling fluids (both particles and filtrates) into the micropore structural networks of oil and gas sandstone producing formations.

The potential for solid invasion damaging the micropore structural networks by reducing the permeability of hydrocarbon-bearing formations or pay-zones and building up filter encrust build up to prevent formation damage have been recognised for many years (Collins and Thaemlitz, 2014). However, designing drilling fluids for minimal formation damage in the near-wellbore area is still a major challenge due to different opinions regarding the use of solid-free and solid-laden reservoir drilling fluids (RDFs) (Fleming et al., 2020; Vickers et al., 2006). These opinions should be properly scrutinised because, despite the PSD of bridging materials used in RDFs, micro-sized solids that are below 1 μm in size, are commonly found in reservoir rock pore networks. These can cause internal damage within the micropore structural networks through the formation of internal filter encrust near surface pores after interaction with the varying clay minerals. The internal filter encrust can be very difficult to remove and can trigger damage reaction mechanisms within the micropore structural networks of producing sandstone reservoirs (Francis et al., 1995; Doane et al., 1999).

Zhang et al. (2020a) studied the effect of water and alkali sensitivity on formation damage mechanism in clay enriched Dongping Bedrock reservoir located in Qaidam Basin. Zhang et al. (2020a) observed that mechanical damage mechanisms are influenced by pore size and can vary from one pore to another. It was observed that small pores were damaged by swelling of mixed-layer illite/smectite clay mineralogy, while large pores suffered from the combined damage of swelling of smectite clay mineralogy and migration of hair-like illite (Zhang et al., 2020a). The findings of Zhang et al. (2020a) indicate that pore throat size is a dominant factor in formation damage reactions associated with migration and swelling of clay minerals and this agrees with the findings of Zhao et al. (2018).

Bennion (2002) observed that the expansion and removal of layers of the clays minerals could lead to a drastic reduction in permeability depending on the amount and location of the clay in the pore system. High salinity fluids, glycols, cationic polymers and amines, and other inhibitors are frequently used to maintain clays of this type in a

contracted or dehydrated state. Clay deflocculation is less understood but more often encountered in sandstone reservoirs than clay swelling. Kaolinitic clay species are an example of non-water-sensitive clay that can be deflocculated in specific situations, and this can be mitigated by preventing excessive cation exchange and sharp or extreme differences in pH (Bennion, 2002).

In another study on chemical mechanisms/rock–fluid interactions, Wuyep et al. (2018) studied the geomechanical impact of various liquids and chemicals used in the petroleum industry on sand failure in oil-/-gas-producing formations located in the Niger Delta Basin; they evaluated the impact of oilfield chemicals (ATMP (AminoTri-Methylene Phosphonic acid) ($C_3H_{12}NO_9P_3$), glycine betaine ($C_5H_{11}NO_2$), and glutaraldehyde ($C_5H_8O_2$) solution) on the geomechanical strength of sandstone reservoir rocks from the Niger Delta using various experimental techniques (mechanical tests, mineral particle size analysis, and analytical tests) to estimate the impact of these chemicals on the rock–fluid damage mechanism. Through clay mineral characterization, they observed a significant growth of chlorite from 6 wt% to 27 wt% and 24 wt% after exposing the core samples to ATMP and glutaraldehyde, respectively, with little or no alteration of the chlorite during exposure to betaine. However, kaolinitic species concentration of 45 wt% in the pre-treatment core samples diminished to 33 wt% and 40 wt% due to exposure to betaine and ATMP, respectively (Wuyep et al., 2018). A slight growth of illitic species from 2 wt% to 4 wt% and 5 wt% after exposure to ATMP and glutaraldehyde, respectively, was recorded; at the same time, the mixed layer (illite + smectite) that moved towards pure smectite with 100% expansion in the pre-treatment core samples was altered from 47 wt% to 58 wt%, 29 wt%, and 27 wt% following treatment with betaine, ATMP and glutaraldehyde respectively Wuyep et al. (2018) concluded that chemical interactions, adsorption, dissolution/precipitation and ionic substitution took place between the oilfield chemicals and the reservoir rocks, which weakened the grain fabrics of the rocks and caused a release of disintegrated grains into the fluid streams. Wuyep et al. (2018) did not consider the varying physicochemical characteristics of the individual clay species observed such as booklet-kaolinite, platy-kaolinite, blocky mixed layer (illite + smectite) or xenomorphic mixed layer (illite + smectite). The current authors note that the shape and size of particles associated with varying physicochemical characteristics of individual clay species may affect the particle-particle interaction, the strength of the formation rock and ultimately affect the extent of formation damage in the sandstone reservoir.

Al-Yami et al. (Al-Yami et al., 2008) studied the effects of the interaction between various water-based drilling fluids and Unayzah-B sandstone reservoir containing clay on formation damage. They investigated the formation damage induced by three different drilling fluids (Mn_3O_4 drill-in fluid, $KCl/CaCO_3/BaSO_4$ drill-in fluid and potassium formate drill-in fluid). They observed that although potassium formate drill-in fluid has low solid content, KCl/Mn_3O_4 drill-in fluid showed the least formation damage compared to the other two drill-in fluids (potassium formate/$CaCO_3$ or $BaSO_4/CaCO_3$ mud systems). They concluded that the poor performance of potassium formate filtrate was because of incompatibility with Unayzah-B formation brine, while that of $BaSO_4/CaCO_3$ drill-in fluid was attributed to trapped barite solids inside the core. The main reason for the better performance of KCl/Mn_3O_4 drill-in fluid was because of the spherical shape and small size of Mn_3O_4 particles, which allowed the particles to be removed by the flow of hydrocarbons. It is noted that, Al-Yami et al. (Al-Yami et al., 2008) did not consider the impact of the interaction of the drilling fluids with the individual clay species on the development and evolution of formation damage in the Unayzah-B sandstone reservoir formation containing varying clay mineralogy. This interaction can cause permeability impairment; however, performances were only judged based on compatibility and sizes of bridging materials present. In another study, Al-Yami et al. (Alyami et al., 2009) studied the effects of water-based RDFs on invading particles and mechanisms of formation damage reaction; they investigated the intensity of damage caused by the weighting materials in three different water-based RDFs (Mn_3O_4 RDF, $CaCO_3$/barite RDF, and KCOOH RDF) used to conduct return permeability tests (Alyami et al., 2009). They observed that the filtrate from KCOOH RDF did not cause migration of kaolinite with booklet-form physiochemical characteristics and environmental scanning electron microscopy (ESEM) and energy-dispersive spectroscopy indicated precipitation of potassium chloride within the pore structures of the reservoir Al-Yami et al. (Alyami et al., 2009) only considered one species, namely booklet-kaolinite and did not consider other individual species of clay minerals of varying physicochemical characteristics, for example, platy-kaolinite, vermicular-kaolinite, and blocky-kaolinite. It is most often the case that kaolinite will detach from rock grain walls, and then migrate and flocculate or deflocculated after interaction with and eroded by drilling fluids.

In a related study, Zhang et al. (2020b) studied how to prevent reduction in the permeability of saline–lacustrine fractured tight oil reservoirs during drilling operations; they observed that the reservoir was composed of a large amount of sensitive clay particles (with the clay content ranging from 5.2 to 30.8 wt% (18.15 wt% on average)); the clay minerals were made up of a mixed layer (illite + smectite) estimated as 2.1 wt% illite estimated as 9.7 wt%, and chlorite, which was dispersed and subsequently migrated to occlude pore throats after interaction with drilling fluids Zhang et al. (2020b) concluded that drilling fluids should be optimized according to fracture developing characteristics of the formation, the impact of salt dissolution on rock properties, and double pressure-bearing ability to plug zone. Zhang et al. (2020b) stated that saltwater sensitivity damage is considered as the essential formation damage mode while drilling. This has supported the fact that increasing salinity can cause formation damage. Nonetheless, Zhang et al. (2020b) like so much of other published research did not pay attention to the individual clay species with varying clay mineralogy. Rather clay mineralogy has been treated as a group.

The major mechanism leading to formation damage is the interactions between solids and fluids in the RDFs with solids and fluids within the micropore structural network of the reservoirs (Francis et al., 1995; Howard, 1995). Formation damage can be a significant factor for ultimately reducing productivity in hydrocarbon-bearing formations (Doane et al., 1999) especially in sandstone reservoirs endowed with varying clay mineralogy such as kaolinite, smectite, illite, mixed layer (illite + smectite) clay mineralogy in the micropore structural networks (Hughes, 1950; Todd et al., 1978; Wilson et al., 2014). These clay minerals are highly unstable/reactive, and for most parts, they exist as pore lining, pore bridging and pore-filling along the micropore structural walls inevitably coming into contact with drilling fluids (both solids and filtrates) that have invaded the micropore structure. The clay minerals with size ranging from 1 μm to 5 μm along the longest diameter (Zhou and Keeling, 2013) are known as "fines'' in the petroleum industry (Hughes, 1950). The fines have significantly altered the transmissibility of oil and gas formation fluids after interacting with invasive RDFs, triggering several types of formation damage reaction mechanisms and thereby posing a major formation damage challenge during drilling operations.

The formation damage reaction mechanisms can occur in combination with other damage mechanisms within the micropore structural networks of sandstone reservoirs containing varying clay minerals, and the resulting formation damage can be severe. For example, clay swelling (a chemical formation damage reaction) coupled with fine migration (a mechanical formation damage reaction). Formation damage reaction due to mechanical mechanism can include nearly all elements of formation damage challenges, such as fine migration, entrainment of external solids, discontinuous dispersion and occlusion of fluids, glazing and smashing, as well as perforations and widening of micropore structures due to small, abrasive solid materials encountered while drilling hydrocarbon-bearing formations. Therefore, it is extremely important to determine and understand the nature of the

formation damage reaction mechanisms likely to occur during a drilling operation to develop appropriate framework for the design and formulation of the drilling fluid (Bishop, 1997).

Experience has shown that the potential for formation damage is highly dependent on the reservoir section to be drilled. The performance of specially formulated drilling fluid can be assessed by testing the fluid on core samples that are representative of the reservoir sections to be drilled. This test is conducted through laboratory experiments tailored to a particular drilling and production programme in an oil and/or gas field as the best approach for FDM/FDC for micropore structural networks of the reservoir sections to be drilled (Bishop, 1997). Various laboratory techniques are used to evaluate formation damage, but the most widely used method is the return permeability method. The return permeability method involves the use of core flood experiment. It measures the initial oil or gas permeability of a natural core or other porous media, and the permeability is also measured after exposing the core sample to a drilling or completion fluid for a given period. Subsequently, the final permeability is measured, allowing for the determination of regained permeability (Vickers et al., 2006; Krueger, 1967; Salimi and Ghalambor, 2011).

Core flood experiments, including determination of initial and return permeability, are widely accepted and used in FDM/FDC measures for the micropore structural network of reservoir sections to be drilled (Kang et al., 2014; Tang et al., 2015; Jin-Gang et al., 2013). Recently, much effort has been directed towards aspects of FDM/FDC measures concerned with the evaluation of sandstone reservoirs via pore-scale/microscopic techniques (Fang et al., 2016; Xu et al., 2016) because productivity impairment, which usually results from a combination of damage reaction mechanisms within the micropore structural networks, can lead to increased Non-Productive Time (NPT), well abandonment, shortened life of fields, high cost/rig time and risk of losing exploration investment. These damage reaction mechanisms are dynamic processes that typically start at a microscopic or pore scale and develop over time to mesoscopic scale, covering several centimetres or even metres of the formation. Therefore, a robust evaluation of formation damage in sandstone reservoirs containing varying clay mineralogy requires techniques that allow simultaneous investigation of the interaction between reservoir rock and drilling fluids at the wellbore face, inner wellbore face, formation face, and inner formation face at typical reservoir conditions. Such evaluation would reasonably demonstrate the impact of the interaction between the varying physicochemical characteristics of the individual clay species observed in the clay mineralogy, such as booklet-kaolinite, platy-kaolinite, blocky mixed layer (illite + smectite) or xenomorphic or anhedral mixed layer (illite + smectite), and newly formulated drilling fluids within the micropore structural networks because the geometry, connectivity and distribution of the micropore structures or pore throats are not linear. The present author is not aware of any existing work in the open literature that is capable of such simultaneous investigation of the impact of drilling fluid – reservoir formation on the nature and severity of formation damage. The general notion in the field of petroleum reservoir engineering that the micropore structures are simple linear spaces between mineral particles can be misleading (He and Stephens, 2011). The obstruction of the micropore structural networks due to the invasion of external solid particles and fluids can extend to a radius greater than 1 foot into the pay-zone of sandstone reservoirs with micropore structural interconnectivity exceeding 25 mD (Epelle and Gerogiorgis, 2020). A major parameter that controls the extent of micropore structural interconnectivity alteration/damage reaction due to corrosion, deflocculation, and flocculation of clay minerals is the geometric disposition of clay minerals inside the micropore structural network.

Previous studies have considered the use of solid-free RDFs (Fleming et al., 2020; Howard, 1995; Downs, 1992; Gao, 2019) or RDFs laden with solids and optimized PSD (Abrams, 1977; Engelhardt, 1954; Vickers et al., 2006) as a means of FDM/FDC for micropore structural networks in general. These studies have treated all the different clay minerals present in the micropore structural network of a reservoir formation as single entity clay group. While the varying physicochemical characteristics of individual clay species have been acknowledged in the literature (Zhang et al., 2020a; Alyami et al., 2009; Hayatdavoudi and Ghalambor, 1996), there is no existing work that explores the interaction of RDFs with individual clay species in the clay minerals found in the micropore structural networks of sandstone reservoirs. Specifically, researchers and industry professionals have yet to consider the design of drilling fluids as an improved FDM/FDC measure for micropore structural networks, specifically targeting (a) kaolinitic hydrocarbon-bearing sandstone reservoirs and (b) mixed layer (illitic + smectitic) and kaolinitic hydrocarbon-bearing sandstone reservoirs. The formulation and design of drilling fluids for minimal formation damage in sandstone reservoirs with varying clay mineralogy is the primary focus of the current research work. For newly formulated drilling fluids to gain industry acceptance, a thorough analysis and assessment are necessary, not only to evaluate safety implications but also to understand the impact on and interaction with the reservoir formation.

Table 1
Characterization of Eocene to Pliocene Agbada Sandstone Reservoir based on spatial disposition and content of varying clay mineralogy.

Clay mineralogy	Discrete particle	Pore filling	Pore bridging	Pore lining
Kaolinite	Sample: 5H	Samples: 8H, 6H		Samples: 6H, 5H
Illite + smectite + Kaolinite	Sample: 3H		Samples: 4H, 7H, 3H	Samples: 4H, 3H, 7H

Table 2
Components for the preparation of PAC-UL water-based drilling fluid (WBDF).

Materials	Concentration	
Deionized Water	500 ml	
Wyoming Bentonite	24 g	4.8 wt%
PAC-UL	2.62 g	0.52 wt%
Xanthan gum	2.1 g	0.42 wt%
KCl	26.2 g	5.2 wt%
NaOH	0.05 g	0.01 wt%
Formaldehyde	1.3 ml	0.1 wt%

2. Experimental equipment and procedures

2.1. Materials

A set of fourteen sandstone core samples from clay enriched Agbada sandstone reservoirs in Tertiary Niger Delta was initially characterized using a combination of scanning electron microscopy, energy dispersive X-ray and micro-computed tomography techniques to determine their suitability for the proposed study. Suitability, in the context of this study, means that these core samples indeed contain clay minerals with varying physicochemical characteristics. A summary of the clay mineralogy is provided in Table 1.

Drilling fluids of varying formulations were designed and tested on sandstone reservoir core samples (Table 1) to determine their impact on productivity impairment. Three different types of drilling fluids were considered: PAC-UL water-based drilling fluid (WBDF), solids-free potassium formate drilling fluid, and halide drilling fluid.

The PAC-UL water-based drilling fluid (WBDF) was formulated for the purpose of benchmarking the performances of the two drilling fluids (potassium formate and traditional halide drilling fluid) used in the field and also used for the formation damage experiments. The additives used to design the base drilling fluid are presented in Table 2 and the particle size distribution of the Wyoming bentonite was determined using MALVERN MASTERSIZER 2000. The particle Size distribution of

Table 3
Fundamental Properties of sodium, potassium, and cesium formate salts (Cabot, 2016).

Brines	Formula	Molecular weight (g/mol)	Solubility at 20 °C/68 °F		Solution Density	
			(mol/L)	(wt %)	(g/cm^3)	(lb/gal)
Sodium formate	NaCHOO	68.01	9.1	46.8	1.33	11.1
Potassium formate	KCHOO	84.12	14.5	75.0	1.59	13.3
Cesium formate	CsCHOO	177.92	–	–	2.30	19.2
Cesium formate monohydrate	CsCHOO.H_2O	195.94	10.7	83.0	2.30	19.2
Formate ion	$CHOO^-$	45.02	–	–	–	–

Table 4
Components of additives used for the formulation of the improved halide drilling fluid designs A, B and C.

Name of material	Chemical formula/concentration (weight %)	Molecular weight (g/mol)	Included in the formulation (YES (Y)/NO (N))		
			A	B	C
Sodium chloride	NaCl (5)	58.44	Y	N	Y
Sodium Bromide	NaBr (5)	102.89	N	Y	Y
Potassium Chloride	KCl (5)	74.55	Y	Y	Y
Calcium Carbonate	$CaCO_3$ (5)	100.09	Y	Y	Y
2-hydroxypropane-1,2,3-tricarboxylic acid	$C_6H_8O_7$ (2)	192.12	Y	Y	Y
Poly (oxy-1,2-ethanediyl), a-butyl-mega-hydroxy	$C_8H_{16}O_3$ (2)	160.21	Y	Y	Y
Propylene glycol	$CH_3CH(OH)CH_2OH$ (1)	76.09	Y	Y	Y

Table 5
Properties of crude oil in S-4 and K-3 Oilfields.

Specific Gravity	Approximately +35 to +45°
Flashpoint	60 °C.
Viscosities	0.863 cP to 12.13 cP
Colour	Dark brown to black

Wyoming bentonite, which was used as the weighting material, was analysed simultaneously with the pore throat size distribution. The particle size distribution of the Wyoming bentonite is in the range of D_{10} = 7.856 μm and D_{50} = 28.455 μm and D_{90} = 66.615 μm, with an average particle surface area of 370–486 g/m^2 and mass density of 15–1.8 g/cm^3.

The second reservoir drilling fluid used in this study is potassium formate drilling fluid. The formate drilling fluids can afford different values of fluid densities (see Table 3) needed in the drilling of reservoir sections with a wide range of pore pressure without additives. Another aspect of the investigation in this study is connected to the use of drilling fluids' designs that are solid free such as potassium formate (Table 3) as an alternative to the traditional halide drilling fluids that are laden with solids.

The third drilling fluid used during this study is the traditional halide drilling fluids. The properties of conventional halide drilling fluid have been improved in this study. The components of the additives that have been used to design the varying formulations of the halide drilling fluid designs (A, B and C) are presented in Table 4. The mixtures used to formulate the halide drilling fluid designs A, B, and C contain sodium chloride, potassium chloride and sodium bromide, along with other additives. Halide drilling fluid A was formulated using mixtures of sodium chloride and potassium chloride, along with other additives. Halide drilling fluid B was formulated using mixtures of sodium bromide and potassium chloride, along with other additives, while halide drilling fluid C was formulated using mixtures of sodium chloride, potassium chloride, and sodium bromide with other additives (Table 4). The crude oil from the oil field being studied has a characteristic dark brown to black colour. The API specific gravity (API) and other vital properties of the oil from the field are shown in Table 5.

To obtain a mineral oil with approximately the same viscosities as the crude oil from the two oil wells, a specialist blending of two types of oil (silicon-based and mineral oil) was carried out to formulate a mineral oil with a viscosity of 12 cP, which was then used for the formation damage return permeability tests. Polydimethylsiloxane having a viscosity of 20 cP provided the required blend with diesel having a viscosity of 5 cP in a ratio of 17:83 by volume, respectively.

2.2. Equipment

In this study, a formation damage test rig for the return permeability test suitable for typical reservoir conditions was developed, designed, built, and commissioned. The formation damage test rig setup consists of four main elements: (i) the upstream system, (ii) the formation damage vessel/core holder, (iii) the instrumentation and data acquisition system. A schematic process and flow diagram showing the connections between the components in the upstream system is provided in Fig. 1.

The formation damage vessel designed and fabricated for the current study can accommodate core samples of varying lengths, ranging from 25.4 mm to 85 mm, and is suitable for the simultaneous application of equal confining and axial pressure. It was built in the engineering workshop of the University of Aberdeen to determine the initial and return permeability of a chosen hydrocarbon reservoir using core samples of varying clay mineralogy and lengths.

The XRD powder diffraction machine was used to identify the phases and composition of clay minerals, both in terms of bulk mineralogy and clay fraction, present in the core samples. The XRD analysis was carried out in the laboratory of X-ray Mineral Services Ltd in Colwyn Bay in the UK. The X-ray diffraction pattern of the varying clay mineralogy was determined with Philips' X-ray diffraction Spectro goniometer equipped with a PW1730 generator. X-ray radiation was provided by a copper target (Cu-anode 2000W). A High-intensity X-ray tube operated at 40 kV and 20 mA. The PW1050 graphite monochromator allows the reading of diffraction angles to ±0.002°.

The SEM equipment was a handy tool in studying the detrital and authigenic clay mineralogy of the sandstone samples and their spatial disposition and structures within the pore network. The SEM analysis was carried out with SEM equipment in the Aberdeen Centre for Electron Microscopy Analysis and Characterization (ACEMAC). The subsamples were coated with carbon in a Q150T Turbo-Pumped Sputter Coater/Carbon Coater.

The micro-CT scanning equipment was used for 3D characterization of the pore throat size distribution of the sandstone reservoir core samples on a micro-scale, which was used for the design of bridging particles used in the RDF. The 3D characterization of the micro-scale pore throat distribution was carried out in this study through direct imaging of the sandstone reservoir core samples using the Nikon XTH 225 ST micro-computerized tomographic machine located in the School of Engineering Fraser Noble Building, University of Aberdeen. The direct imaging technique has been used to characterize the distribution and texture of pore throats at a micro-scale in hydrocarbon-bearing sandstones (Bin et al., 2013; Dong and Blunt, 2009).

2.3. Procedures

2.3.1. Core sample preparation

Preservation of the mineralogy and pore throat network during the

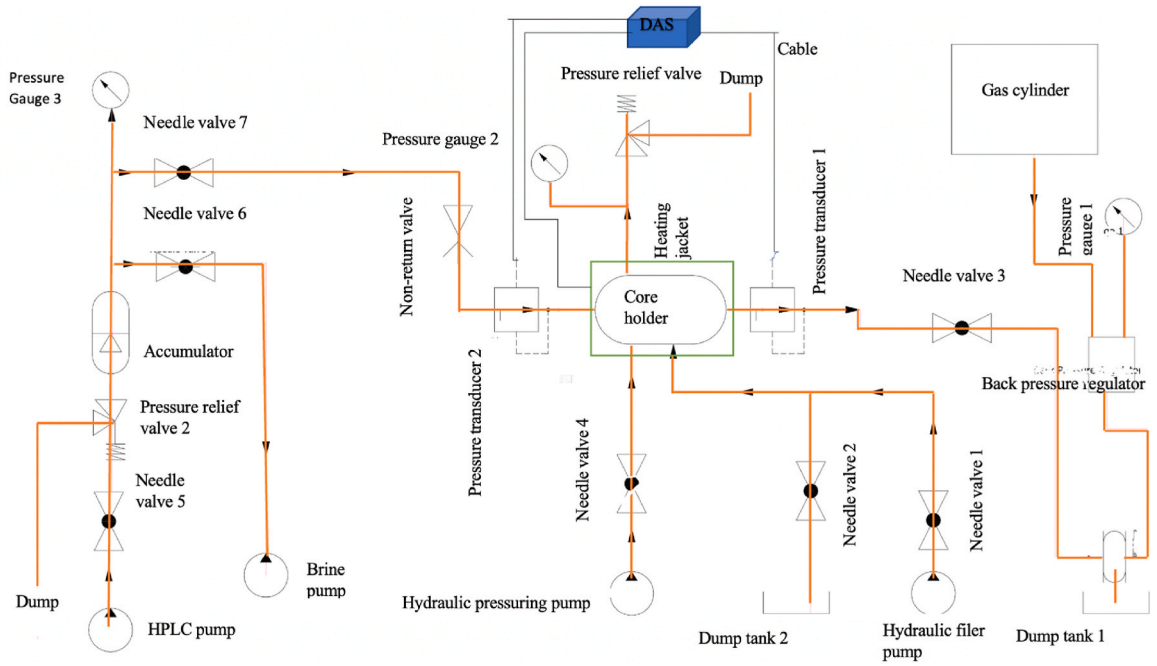

Fig. 1. Process, flow, and instrumentation diagram of the formation damage test rig.

extraction of the fluids in the core samples is a very important aspect in core analysis (CoÅŸkuner and Maini, 1990; Schwark et al., 1997). In this study, sub-samples were cleaned with toluene and chloroform/methanol azeotropic solvent. However, the chloroform/methanol azeotrope cleaning of core samples gave the best result in terms of effective cleaning and alteration of pore structures. Hence, chloroform/methanol azeotrope was selected for cleaning the core samples. The core samples were cleaned in a Soxhlet extractor containing a mixture of chloroform and methanol in a ratio of 87:13 by volume, respectively. This cleaning method was used by French et al. and has been documented in related literature (French et al., 1995). A humidity oven set up to a temperature of 63 °C with a relative humidity of 35% was used to dry the core samples after cleaning due to the presence of clay minerals in the core samples. The cleaned, dried core samples were placed in a pressure saturator and evacuated for 24 h. After evacuation, synthetic formation brine was introduced into the saturator until all the plugs were fully submerged in the brine, and a pressure of 2000 psi was gradually applied for the plugs to become brine saturated for an average time duration of 24 h (Francis et al., 1995).

2.3.2. X-ray powder diffraction analysis

Two types of tests (bulk mineralogy and clay fraction) were carried out employing X-ray powder diffraction (XRPD) using the identification and quantification of polycrystalline materials. Bulk samples were wet ground for 12 min in ethanol using a Micronising mill and sprayed dry to obtain x-ray diffraction powder specimens. X-ray powder diffraction (XRPD) patterns were analysed between 4.5° and 75° 2θ (theta) at a step size of 0.013 and nominal time per step of 0.2 s (continuous scanning mode) using radiation from a Copper anode at 40 kV, 40 mA.

Quantitative analysis was made by a normalized total pattern reference intensity ratio (RIR) method as described in (Omotoso et al., 2006). Expanded uncertainty using a coverage factor of 2, i.e., 95% confidence, was given by $X \pm 0.35$, where X is the concentration in wt.% (Hillier, 1999). The analysis was performed taking into account that for phases present at the trace level (<1 wt%), there may also be uncertainty as to whether the phase is genuinely present in the sample since this is both phase and sample dependent. The clay fractions of <2 μm were obtained by timed sedimentation, prepared as an oriented mount using the filter peel transfer technique and scanned between 2° and 45° 2θ in the air-dried state, after glycolation, and after heating to 300 °C for 1 h. The identified clay minerals were quantified using a mineral intensity factor approach based on calculated XRPD patterns.

2.3.3. Scanning electron microscopy (SEM) analysis

To evaluate formation damage in reservoirs with varying clay mineralogy, it is necessary to investigate the interaction between formation rock and drilling fluids at different interfaces. Subsamples of approximately 1 cm were prepared for this purpose. Trims were taken from the samples before and after core flood tests for scanning electron microscopy (SEM) studies. The SEM scans were conducted at an accelerating voltage of 15 kV and magnifications of×500 and ×100, with an aperture size of 50 μm. Details of the procedure of the SEM are provided in (Danilatos and Robinson, 1979).

SEM Photomicrographs were processed using ImageJ with a known scale determined based Horizontal Field of View (HFOV) of squares in nanometres per pixel. So that grain measurements can be returned in nanometres since ImageJ does not return measurements less than one unit of the scale. Therefore, grain size measurements were carried out for particle size (clay, silt and sand) based on Feret diameters by taking the average of multiple measurements along different grain axes. Feret diameters for grain size at 1 phi intervals were calculated by summing up the diameter in each class interval. Additionally, the percentage of Feret diameter in the class interval was determined as a measurement of the percentage for each grain size class.

The grain size characteristics were compared, and sorting was determined by using the variation in the percentage of sand, silt and clay contents.

Grain size and sorting were measured by determining the Feret diameters of all grains within one phi size class. The total number of grains was then multiplied by the phi class size and the percentage within each class was determined.

2.3.4. Micro computer tomography analysis

The objective of the 3D analysis is to acquire the pore throat size distribution. The procedure followed during the analysis process involves thresholding, filtering, phase segmentation, labelling and object separation (Hu et al., 2015). The pore throat size distribution commonly selected are the largest micropore structures (D90), the medium

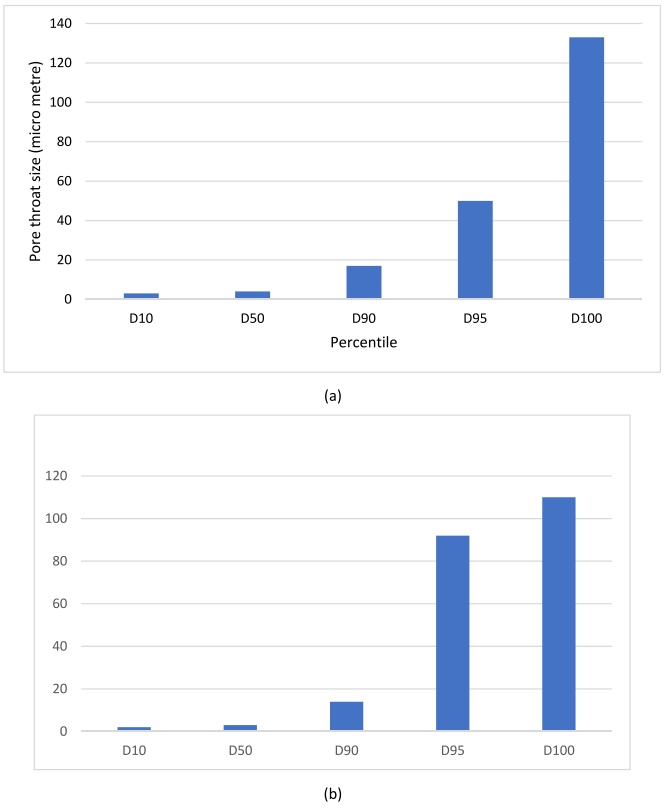

Fig. 2. Pore throat size distribution of Eocene to Pliocene Agbada hydrocarbon sandstone reservoir- (a) S-4 (b) K-3.

micropore structures (D50) and a small micropore structures (D10) (Vickers et al., 2006).

Micro-CT 3D images and data of a 1-inch diameter, 1-inch height core sample were analysed using Avizo 9.0[1] software to determine the pore throat size distribution. The images underwent denoising/smoothing and image segmentation processes. Pore space and rock matrix were separated, and further steps involved separating pores from each other, computing the skeleton and distance map, applying the "regional maximal" function, and labelling the distance map. Separation zones were computed using the labelled distance map through the watershed operation. The separated and labelled pore space surface was generated, and statistics (Fig. 2a & b) were obtained using the Measure/Surface Area Volume module, providing information about pore bodies and throats. The 3D pore space measurement of the pore throat size distribution of the Eocene to Pliocene Agbada sandstone reservoir was required to design the accurate bridging particle size distribution needed for the formulation of the Reservoir Drilling Fluids (RDF). The importance of using the pore throat size distribution data of representative cores of hydrocarbon reservoirs in the design of RDF has been discussed extensively (Darley and Gray, 2011; Zhang et al., 2014).

In this study, the pore throat size distributions of the Eocene to Pliocene Agbada sandstone reservoir (in K-3 and S-4 oilfields) have been determined and is presented in Figures: (2a and 2 b). It is observed that there are significantly higher proportion of pores present in D95 than in D90 (see Fig. 2a & b); hence D95 was used to construct the bridging package.

2.3.5. PAC-UL water-based drilling fluid (WBDF)

The base drilling fluid was prepared by mixing 24 g of Wyoming bentonite with 500 ml of distilled water, using the Hamilton Beach Single Spindle Mixer. Before new additives were added into the mixture, the mixture was thoroughly blended for about 5 min to ensure adequate dispersion of the additives. An ultrasonication process in the ultrasonic bath at a frequency of 25 kHz and input power of 450 W for a 1-h period was performed to reduce the ageing time for the base drilling fluid and allowed the tests to be carried out on the same day (Dejtaradon et al., 2019).

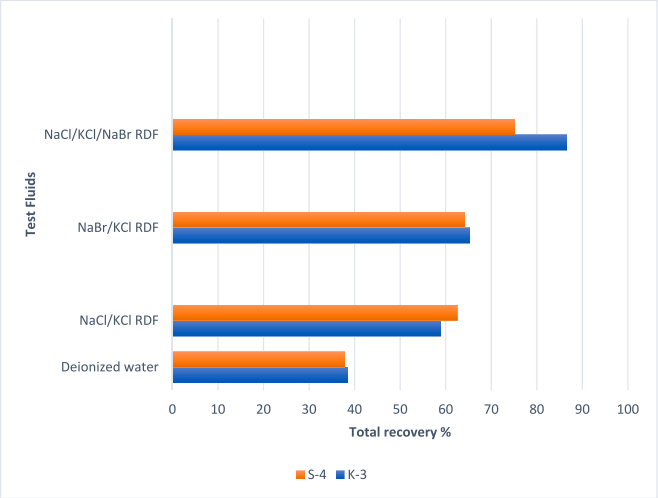

Fig. 3. Dispersion test results for S-4 and K-3.

2.3.6. Halide drilling fluids' hot rolling dispersion test

Hot rolling dispersion test was carried out to assess the dispersion tendency of the reservoir rock formation under consideration in each of the three halide brine formulations The dispersion test utilized sandstone core samples from K-3 oilfield (containing only varying kaolinite clay mineralogy) and S-4 oilfield (containing varying kaolinite & mixed-layer (illite + smectite)). The test evaluated the potential impact on and interaction of these kaolinitic clay mineralogy and mixed layer (illitic + smectitic) and kaolinitic clay mineralogy with the varying formulations of the halide drilling fluids' designs A, B and C (Table 4).

The four sandstone core samples were prepared to obtain pieces of a specific size (1–3 mm) (Gomez et al., 2015) and weighing them. The dispersion test was performed by exposing known weight of the sandstone core samples with sized pieces (1–3 mm) to the halide drilling fluids (Table 4) in a conventional roller-oven cell. This provided long-term exposure of the sandstone core samples to the fluids under mild agitation conditions. Under such conditions, dispersion of the clay fines into the fluid occurs depending on the tendency of the clay mineralogy to disperse and the inhibitive properties of the drilling fluid (Abbas et al., 2018). The fluid and sandstone pieces were rolled together in a roller oven for 16 h at 150 °C. The fluids were allowed to cool to room temperature. Subsequently, the fluid was poured out over a 20-mesh sieve, and the retained sandstone core samples were recovered, washed, weighed, and then dried overnight at 110 °C. The samples were then re-weighed to determine the moisture content of the sandstone core samples and the recovery percentage of the sandstone core sample. Deionized (DI) water was used as a benchmark to compare with these halide drilling fluid designs A, B, and C in the hot rolling dispersion test. The ratio between the final weight after drying and the initial weight before exposure to the fluid served as a measure of the recovery, while the difference between the weights after exposure to the fluids but prior to drying and after drying provided a measure of the moisture content. A high value of recovery indicates high-quality inhibition and low-quality dispersion. A total of eight hot rolling dispersion tests were performed (four tests each for K-3 and S-4).

The result of the hot dispersion test is shown in Fig. 3. Therefore, NaCl/KCl/NaBr-RDF design (Table 4) was more effective and helped to control the dispersion of the reactive varying clay mineralogy. Consequently, the halide drilling fluid design option C (Table 4) was selected as the drilling fluid candidate for formation damage study.

Table 6
Rheological properties of drilling fluids used in this study.

	Halide drilling fluid	PAC-UL WBD fluid	K-formate drilling fluid
Plastic viscosity (PV)	20 cP	15 cP	18 cP
Gel strength 10 s	9 lb/100 ft^2	10 lb/100 ft^2	18 lb/100 ft^2
Gel strength 10 min	13 lb/100 ft^2	12 lb/100 ft^2	32 lb/100 ft^2
Yield point (YP)	31 lb/100 ft^2	27 lb/100 ft^2	19 lb/100 ft^2

The rheological properties of the drilling fluids were determined using OFITE viscometer model 900. The rheological properties of the drilling fluids used in this study are presented in Table 6.

2.3.7. Pre-treatment analysis of core samples

The mineralogy and pore network analysis of the formation rock from oil fields K-3 and S-4 is presented in Table 1. Before conducting the formation damage test, petrophysical properties such as permeability to mineral oil and porosity were determined for the core samples. To determine the initial permeability to mineral oil, the core samples were identified at the formation-end (FE) and wellbore-end (WE) and sealed in a thin-walled Viton sleeve using end caps. The sealed samples were placed in a formation damage vessel connected to upstream and downstream flowlines. The annulus of the core holder was filled with pressuring fluid, and an overburden pressure of 4236 psi (29.2 MPa) was applied. The vessel was heated to 107 °C and flooded with mineral oil from the formation face to the wellbore face to simulate oil production. The flooding lasted 24 h at a low flow rate (0.1 ml/min to 0.5 ml/min) to prevent fines migration, while continuously recording upstream and downstream pressures. (Krueger, 1967).

The core flood test was stopped when the effluent from the wellbore end consisted solely of mineral oil and pressure values had stabilized, indicating irreducible brine saturation (S_{wi}). The original permeability at irreducible brine saturation was determined using Darcy's equation and the stabilized differential pressure.

After reaching irreducible brine saturation, the core plugs were removed, fully immersed in mineral oil in sealed containers, and stored under an argon blanket at 107 °C in an oven. This ensured the core samples equilibrated with reservoir conditions before further analysis and formation damage experiments (French et al., 1995).

2.3.8. Formation damage post-treatment analysis

A post-treatment analysis became necessary to aid in visualizing permeability alterations within the micropore structure of the sandstone reservoir core sample after interaction with the reservoir drilling fluids.

Return permeability measurement was undertaken by carrying out mineral oil flooding of the drilling fluid saturated core samples. The drilling fluid-saturated core sample was placed inside the formation damage vessel, and the core flooding process described in the preceding section was repeated, but this time mineral oil was used as flooding medium. The mineral oil was injected into the core sample from FE to WE to depict the production of oil from the reservoir after formation damage due to drilling fluid interaction with the formation rock had occurred. This involved pumping the mineral oil through the sample at a constant flow rate initially, followed by a series of increasing flow rates (Krueger, 1967); this is known as drawdown. Throughout the drawdown phase, the pressure across the core sample was measured, and the pressure response was used to describe the clean-up behaviour of the rock, fluids, and formation damage. Therefore, the technique favoured to replicate the drawdown or natural clean-up is the constant flow rate or constant incremental flow rates while measuring the pressure differential along the length of the core sample (Krueger, 1967; Salimi and Ghalambor, 2011). The injection of mineral oil was stopped when a constant differential pressure was attained, and the core was subsequently removed from the vessel.

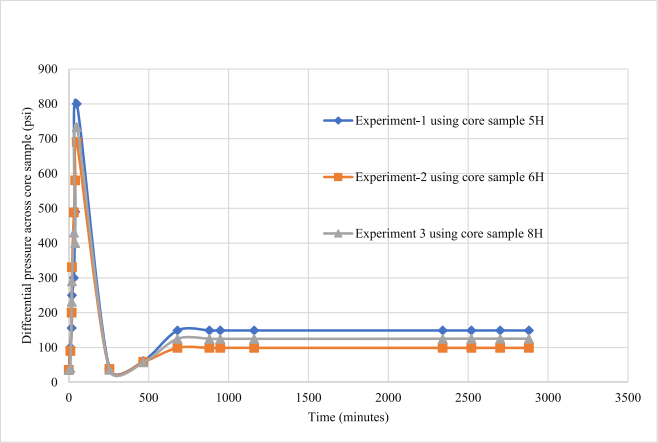

Fig. 4. Differential pressure – time response curves for core samples (5H, 6H, 8H respectively) from K-3 oil field at a flowrate of 0.5 ml/min and overburden pressure of 4236 psi.

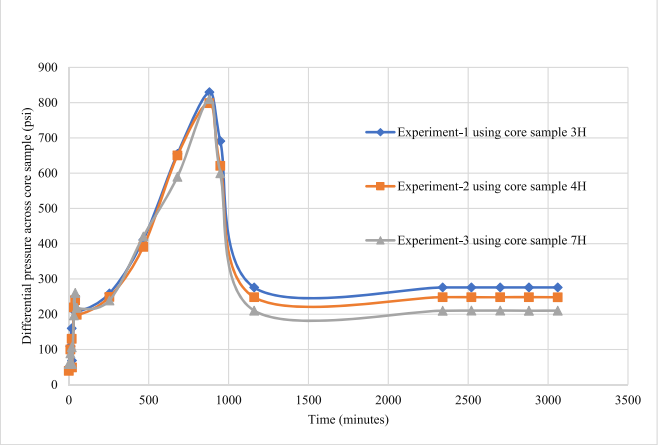

Fig. 5. Differential pressure – time response curves for core samples (3H, 4H, 7H respectively) from S-4 oil field at a flowrate of 0.5 ml/min and overburden pressure of 4236 psi.

3. Results and discussions

This section presents the results of the six return permeability tests conducted on the kaolinitic & mixed layer (illitic and smectitic) sandstone reservoir and the kaolinitic sandstone reservoir using three drilling fluids: formate drilling fluid, improved halide drilling fluid, and water-based drilling fluid. The six core samples (3H, 4H, 5H, 6H, 7H & 8H) used were sandstone reservoir cores, with 5H, 6H, and 8H acquired from K-3 Oilfield, and 3H, 4H, and 7H acquired from S-4 Oilfield in Niger Delta. The purpose of the experiment was to assess, quantify, and characterize the effect of the interaction between drilling fluids of varying formulations and reservoir sections containing kaolinite and mixed layer (illite and smectite) or only kaolinite on permeability impairment.

All experiments were repeated three times to ensure repeatability, and error bars were plotted from the average data obtained.

3.1. Determination of core samples' initial permeability

The initial permeability of core samples from K-3 and S-4 oil fields was determined during the initial core flooding with mineral oil. The differential pressure (ΔP) – time response curves were established for the core samples: (5H, 6H, and 8H) acquired from K-3 Oilfield and (3H,

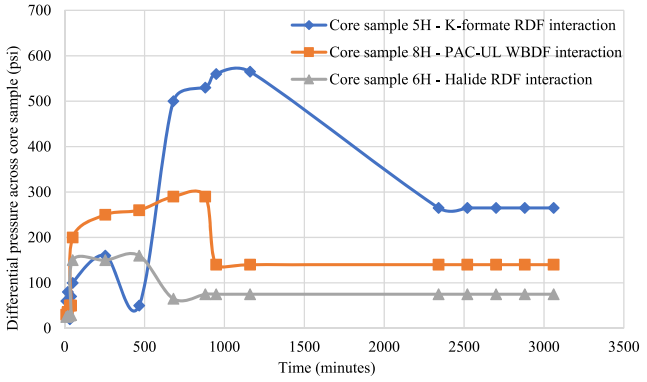

Fig. 6. Representative differential pressure - time response curves for K-3 core samples (5H, 6H, 8H) – drilling fluid interaction with core samples exposed to K-formate RDF showing severe decline in initial permeability lower than those of core samples exposed to PAC-UL WBDF at temperature of 107 °C and overburden pressure of 4236 psi and flowrate of 0.5 ml/min.

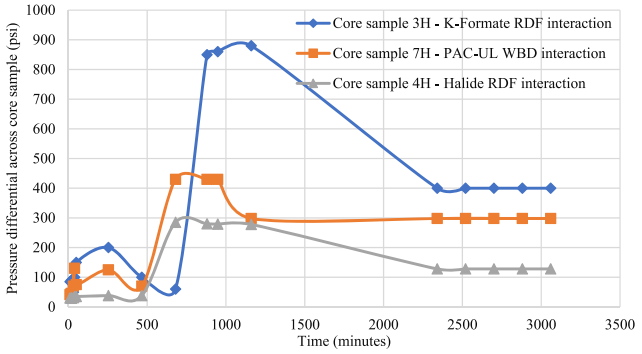

Fig. 7. Representative differential pressure - time response curves for S-4 core samples (3H, 4H, 7H) – drilling fluid interaction with core samples exposed to Halide RDF showing initial permeability higher than those of core samples exposed to PAC-UL WBDF at temperature of 107 °C and overburden pressure of 4236 psi and flowrate of 0.5 ml/min.

4H and 7H) from S-4 Oilfield, tested during the initial core flooding with mineral oil. Before doing the initial core flooding the optimum flow rate was determined as 0.5 ml/min. Since (ΔP) – time response depends on overburden pressure, the reservoir pressure (4236 psi) commonly encountered in K-3 and S-4 Oilfields was used. The three curves for each core from K-3 Oilfield were superimposed (Fig. 4) likewise in Fig. 5 for S-4 Oilfield.

The differential pressure (ΔP) – time response graphs presented in Figs. 4 and 5 were obtained using sandstone cores samples from K-3 and S-4 oil fields. However, ΔP across the samples from the K-3 oil field was significantly lower than ΔP across core samples from the S-4 oil field. There are three distinct stages in Figs. 4 and 5. First, there was an initial rapid increase in the values of ΔP, and this can be attributed to the equilibration process between the mineral oil and clay mineralogy within the pore structural network. This equilibration process was complicated across core samples from the S-4 oil field due to the presence of kaolinitic and mixed layer (illitic + smectitic) clay mineralogy, which made the pore structures tortuous (Fig. 5). The second stage is characterized by a rapid decrease in values of ΔP, which begins at the peak of the equilibration process. The lowest values of ΔP attained in Fig. 4 indicate pore structural networks that have good interconnectivity compared to those in Fig. 5. Additionally, the third stage shows a stable ΔP was quickly and more easily attained across core samples from the K-3 oil field (Figs. 4 and 5), leading to variation in the values of initial permeability determined for both core samples from K-3 and S-4 oil fields.

It's important to note that large pores do not necessarily result in high permeability or transmissibility of hydrocarbon reservoirs. However, high permeability indicates strong connectivity between pores via pore throats, as depicted by the lower values of ΔP in Fig. 4. This observation is supported by the pore throat size distribution data shown in Fig. 2.

3.2. Determination of formation damage return permeability

The representative *ΔP* – time response graphs were established during the core flooding with each of the three drilling fluids using K-3 Oilfield's core samples (5H, 6H, 8H) and (b) S-4 Oilfield's core samples (3H, 4H, 7H). Each figure has three curves, one for each of the three drilling fluids with the core sample label identified. The three curves on each Figure were superimposed, and important parameters including the overburden pressure (4236 psi), temperature (107 °C) and flowrate 0.5 ml/min were implemented during the core flood tests. These were needed to show the effect of drilling fluid formulation on the response, because one of the main aims of the project is drilling fluid – reservoir rock interaction.

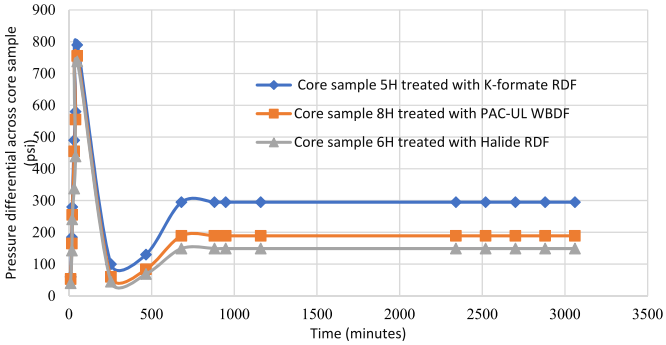

Fig. 8. Representative differential pressure – time response during back production for K-3 core samples (5H, 6H, 8H) at temperature of 107 °C and overburden pressure of 4236 psi and flowrate of 0.5 ml/min.

The representative *ΔP* – time response during back production, that is during the core flooding with mineral oil from the formation end for core samples: (5H, 6H, 8H) and (3H, 4H, 7H). Each figure has three curves, one for each of the three drilling fluids and the core sample label identified. The three curves on each figure have been superimposed at the overburden pressure (4236 psi) temperature (107 °C) and flowrate of 0.5 ml/min.

The representative differential pressure *ΔP* versus time response during the interaction between the three different drilling fluids with varying formulations (namely PAC-UL water-based drilling fluid (WBDF), potassium formate RDF and Halide RDF) and the K-3 core samples (5H, 6H, 8H) and S-4 core samples (3H, 4H, 7H) are presented in Figs. 6–7. The average initial permeability of core samples (5H, 6H, 8H) from K-3 and (3H, 4H, 7H) from S-4 oil fields determined in this study is within the range of the values of initial permeability (750–5200 mD) for oil fields in Agbada sandstone reservoirs of the Niger Delta Basin contained in published literatures (Jev et al., 1993; Poston et al., 1983; Obiora et al., 2016; Amigun and Odole, 2013). However, the initial permeability of core samples was reduced in both S-4 and K-3 Oilfields a result of RDF-reservoir rock interaction (Figs. 6 and 7) but there was a severe decline in initial permeability of core samples exposed to K-formate RDF compared to halide RDF (Figs. 6 and 7).

In Fig. 6, the values of differential pressure *ΔP* for K-3 core samples (5H, 6H, 8H) are lower compared to its corresponding values in Fig. 7 for S-4 core samples (3H, 4H, 7H). This suggests that the drilling fluid-reservoir rock interaction in the K-3 oil field may have caused reduced alteration of micropore structure connectivity and ultimately minimal

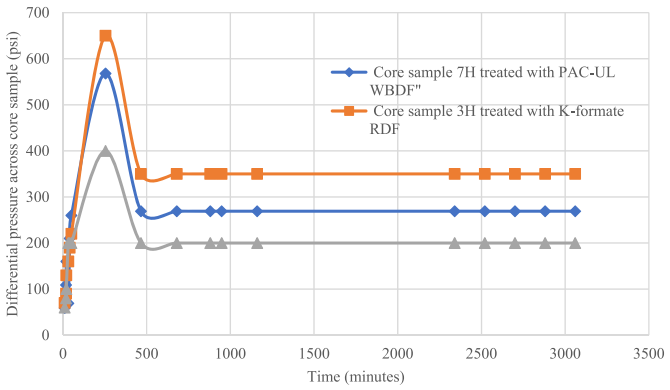

Fig. 9. Representative differential pressure – time response during back production for S-4 core samples (3H, 4H, 7H) at temperature of 107 °C and overburden pressure of 4236 psi and flowrate of 0.5 ml/min.

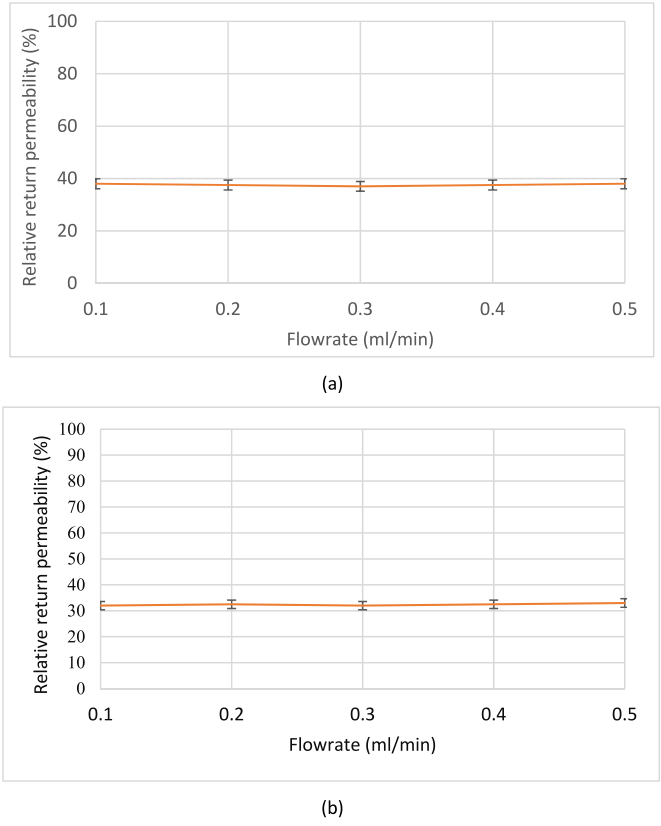

Fig. 10. Average return permeability versus flowrate (a) for core sample 8H from K-3 oil field (b) for core sample 7H from S-4 oil field at overburden pressure of 4236 psi and temperature of 107 °C.

formation damage, in comparison to the drilling fluid interaction with S-4 core samples. The micro-structural spatial disposition of clay mineralogy for K-3 core samples (5H, 6H, 8H) are pore lining and pore filling, while for S-4 core samples (3H, 4H, 7H), are pore bridging (Table 1).

The representative differential pressure – time response during back production, that is during core flooding with mineral oil from formation end (FE) for K-3 core samples (5H, 6H, 8H) and S-4 core samples (3H, 4H, 7H) are presented in Figs. 8 and 9, respectively. In Fig. 8, the representative differential pressure values for K-3 core samples (5H, 6H, 8H) are lower compared to S-4 core samples (3H, 4H, 7H), indicating a lower degree of damage to permeability. This difference can be attributed to the impact on the damage of permeability. S-4 core samples (3H,

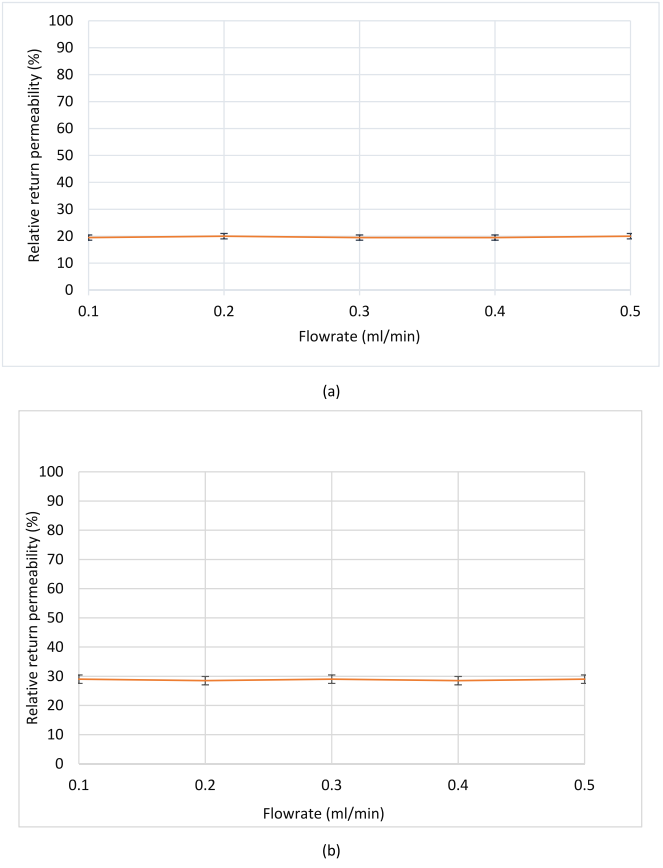

Fig. 11. Average return permeability versus flowrate (a) for core sample 3H from S-4 oil field and (b) for core sample 5H fromK-3 oil field. at overburden pressure of 4236 psi and temperature of 107 °C.

4H, 7H) exhibit a higher reduction in permeability due to a combination of damage mechanisms, including swelling and fine migration. In contrast, the dominant damage mechanism in K-3 core samples (5H, 6H, 8H) is migration. Therefore, achieving return permeability maybe more easily attainable in the K-3 oil field. Return permeability was determined by calculating the ratio of the measured return permeability during back production to the initial permeability before formation damage.

3.2.1. Relative return permeability after treatment with PAC-UL to water-based drilling fluid

The plot of the relative return permeability (%) versus flow rate for the three core samples (5H, 6H, 8H) from K-3 Oilfield was established at a drawdown range of 0.1–0.5 ml/min hence, error bars have been included on the graphs and likewise for the three core samples (3H, 4H, 7H) from S-4 Oilfield at the overburden pressure of 4236 psi and temperature of 107 °C.

The return permeability is presented in Fig. 10a for core sample 8H from K-3 oil field and in Fig. 10b for core sample 7H from S-4 oil field. Both core samples were tested with water-based drilling fluid PAC-UL.

The result in Fig. 10a indicates that the base drilling fluid did not perform well. The interaction between the water-based drilling fluid and core sample 8H resulted in a severe decline in permeability. Core Sample 8H showed a 62% loss in permeability, with a return permeability of only 38% (Fig. 10a). Any damage exceeding 30% during a formation damage return permeability test will affect the fluid flow properties of an oil well (Browne and Smith, 1994). However, the return permeability was not up to 50% of the original permeability of the reservoir, as represented by core samples 7H (Fig. 10b). The return permeability tests using water-base drilling fluid PAC-UL and core samples 8H and 7H

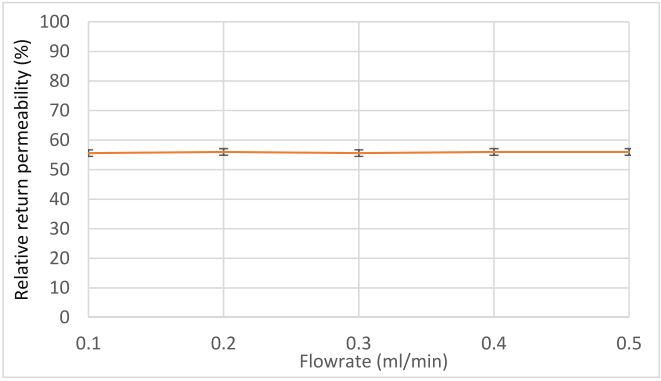

(a)

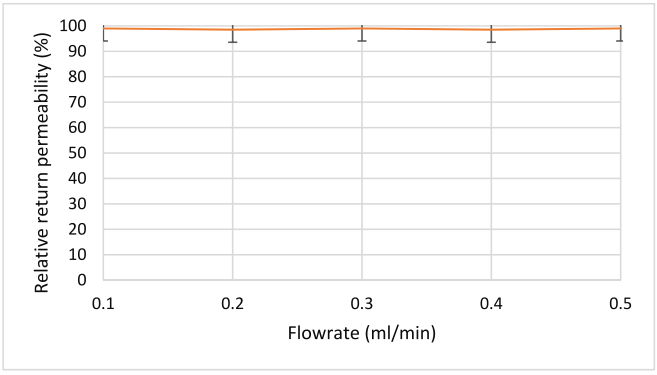

Fig. 12. Average return permeability versus flowrate (a) for core sample 4H from S-4 oil field and (b) for core sample 6H from K-3 oil field at overburden pressure of 4236 psi and temperature of 107 °C.

were conducted to benchmark the performances of the potassium formate and halide drilling fluids in Kaolinitic and mixed layer illitic + smectitic sandstone reservoirs.

3.2.2. *Relative return permeability after treatment with K-formate drilling fluid*

The S-4 core sample 3H and K-3 core sample 5H were exposed to K-formate drilling fluid during the core flooding experiment. The return permeability versus flowrate (ml/min) for S-4 core sample 3H and K-3 core sample 5H are presented in Fig. 11a and b, respectively.

The return permeability test for S-4 core sample 3H showed an 80% permeability damage. On the other hand, in the reservoir represented by K-3 core sample 5H (Fig. 11b), the recovery permeability value was 29%. These low return permeability values suggest that the performance of K-formate drilling fluid may have induced formation damage reactions, possibly involving swelling of smectitic clay mineralogy and migration of kaolinite. A productivity impairment of up to 74% is considered poor performance (Bishop, 1997), and it is likely that both swelling and migration damage mechanisms occurred in S-4 core sample 3H, while migration was the only formation damage mechanism in K-3 core sample 5H. SEM will be used in subsequent subsections to determine the dominant formation damage mechanisms.

The interaction of K-formate RDF with the rock samples (3H and 5H) resulted in the mobilization of colloidal clay particles within the micropore structural network due to an increase in the electrical double layer. As a result, particles were separated from pore surfaces, leading to a reduction in permeability. Similar results have been observed by other authors (Khilar and Fogler, 1987; Khilar et al., 1990; Kia et al., 1987) studying sandstone reservoir rocks.

3.2.3. *Relative return permeability after treatment with halide drilling fluid*

The results of the formation damage return permeability test for

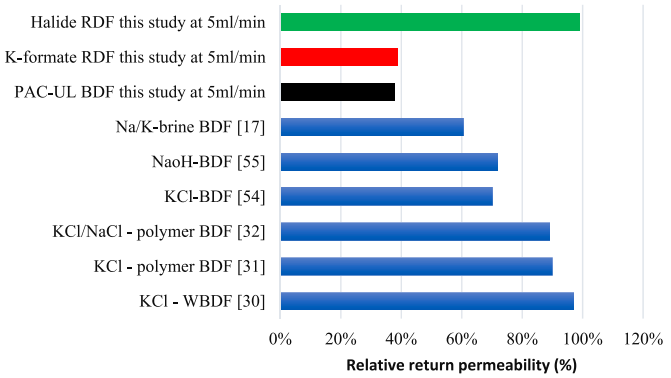

Fig. 13. Comparison of relative return permeability values from various water-based drilling fluids at elevated temperatures and pressures.

improved halide drilling fluid on S-4 core sample 4H and K-3 core sample 6H are presented in Fig. 12a and b, respectively. Fig. 12a indicates that permeability has been severely impaired due to the interaction and impact of the halide drilling fluid on kaolinite along with mixed layer (illite + smectite) reservoir. As shown in Fig. 12a, the reservoir represented by S-4 core sample 4H recovered 56% of its original permeability. The relative performance of the halide drilling fluid in the two different reservoirs is illustrated in the results presented in Fig. 12a and b.

The result presented in Fig. 12b indicates that halide drilling fluid performed well in the kaolinitic reservoir of K-3 due to low retention, resulting in minimum impairment of the reservoir. As shown in Fig. 12b, the return permeability value was 99%.

Drilling fluid damage levels ranging from 0% to 99% permeability reduction have been recorded; however, permeability impairments of less than approximately 50% have minimal effect on reservoir productivity (Browne et al., 1995). The interaction of the halide RDF with rock samples (4H and 6H) resulted in a reduced effective internal surface area of the rock samples, which could be a possible reason for the high return permeability. When the reservoir rock-drilling fluid interaction involves only a small specific surface area of the rock in contact with the fluid, it leads to increased return permeability.

A number of sandstone reservoirs contain interstitial clay mineralogy with varying physicochemical characteristics within their micropore structures. Swelling and dispersion of the clay mineralogy can be responsible for the impairment of the permeability (Gomez et al., 2015). The improved halide drilling fluid showed its best performance when used in a kaolinitic reservoir rock (core sample 6H). This experimental study highlights the importance of blending multiple salts in RDF design to apply the inhibitory control properties of each individual salt. As a result, an improved halide RDF with a robust formulation, comparable to commercially available RDFs and those in other related studies, was achieved, as shown in Fig. 13.

3.2.4. *Effects of water-based drilling fluid PAC-UL on physiochemical alteration of sandstone reservoir with varying clay mineralogy*

The effect of the PAC-UL Base Drilling Fluid on the physicochemical alteration of the clay mineralogy was first to be investigated so reference can be made to it for comparison when investigating the effects of the other RDF types. SEM images was used to assess and determine the formation damage mechanism(s) that helps to explain the return permeability response presented in the previous sections.

Images are presented as 'Before formation damage' for the images taken after the initial core flooding with mineral oil, and 'After back production' to refer to the images taken after the back production. SEM images at Wellbore face and Formation face were taken and a possible reason for the poor performance of the PAC-UL base drilling fluid was further investigated with SEM-EDS analysis and the result is presented in

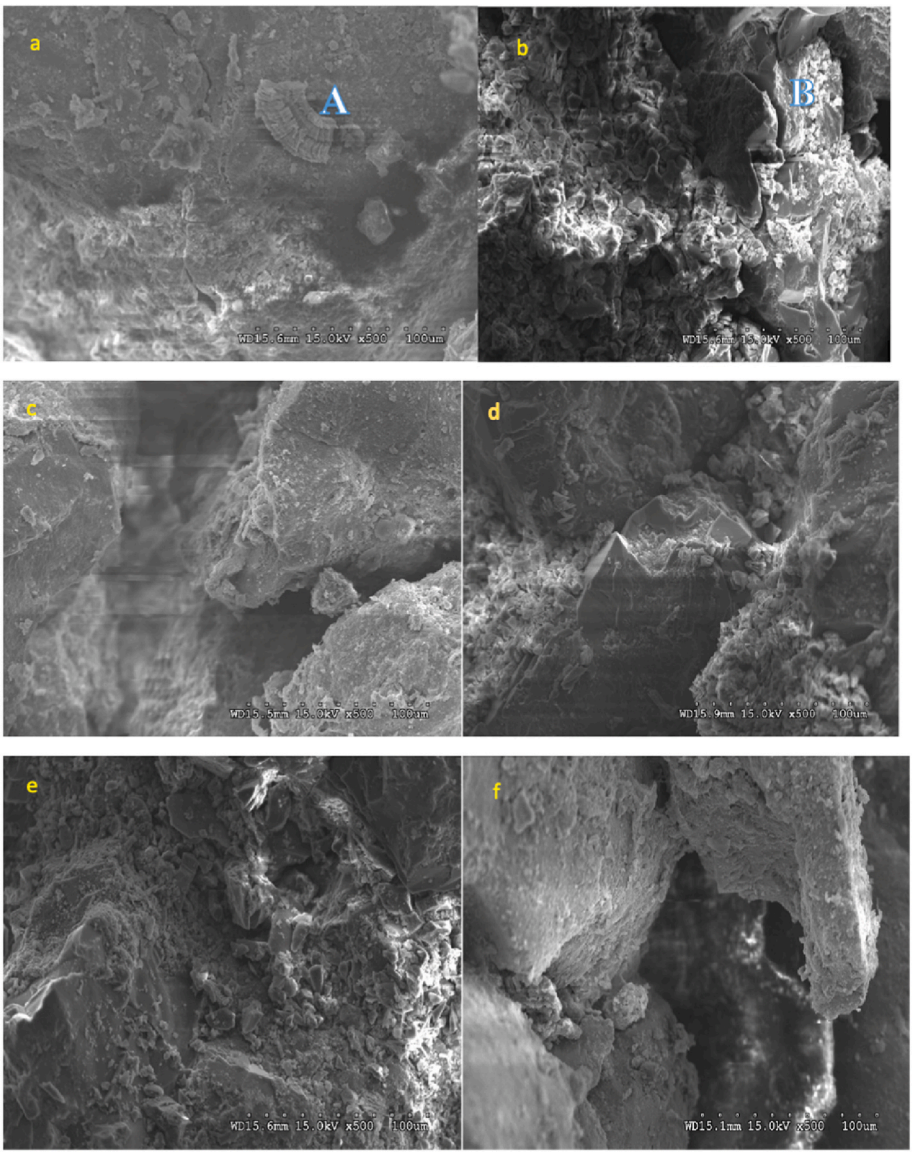

Fig. 14. SEM photomicrographs of K-3 core sample 8H at depth 7526.60 ft showing (a) WE – face (Before), (b) WE - face (After), (c) FE-face (Before), (d) FE – face (After), (e) WE – inside (After) and (f) FE – inside (After). Sites of EDS analysis are indicated A and B.

the following sub sections.

3.2.4.1. Physicochemical alterations at wellbore end (WE) and formation end (FE) of core sample 8H K-3. In this subsection, the physicochemical alterations at the wellbore end (WE) and formation end (FE) are presented. The SEM analysis results for the WE - face (Before formation damage and After back production) are shown in Fig. 14 (a and b). The invasion of drilling fluid solids has contributed to the reduction in permeability (Fig. 10a). The SEM analysis results for the formation end (FE) (Before formation damage) and (After back production) are presented in Fig. 14 (c and d respectively), and SEM analysis results for the WE – 2 mm inside (After back production) and FE - 2 mm inside (After back production) are shown in Fig. 14 (e and f). The dominant formation damage mechanisms are destabilization and migration of clay minerals. The pore structural networks have been occluded by deflocculated and migrating clay minerals after interaction with constituents of water base drilling fluid PAC-UL (Figures: 14 - d, e, and f), resulting in the observed low relative return permeability in Fig. 11a.

The invasion of drilling fluid solids is evident in the WE – face (After back production - Fig. 14b) and WE – 2 mm inside (After back

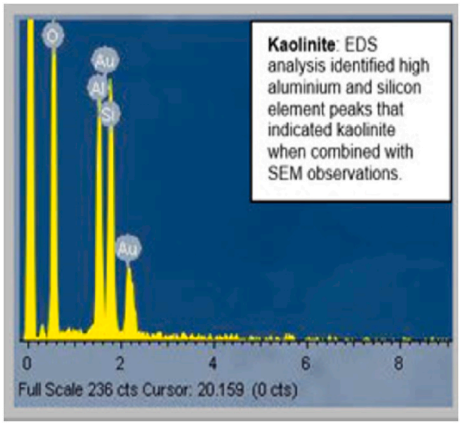

Fig. 15. EDS at location A of Fig. 15 showing high peaks for Silicon and Aluminium, which is indicative of kaolinite. Location B has similar result.

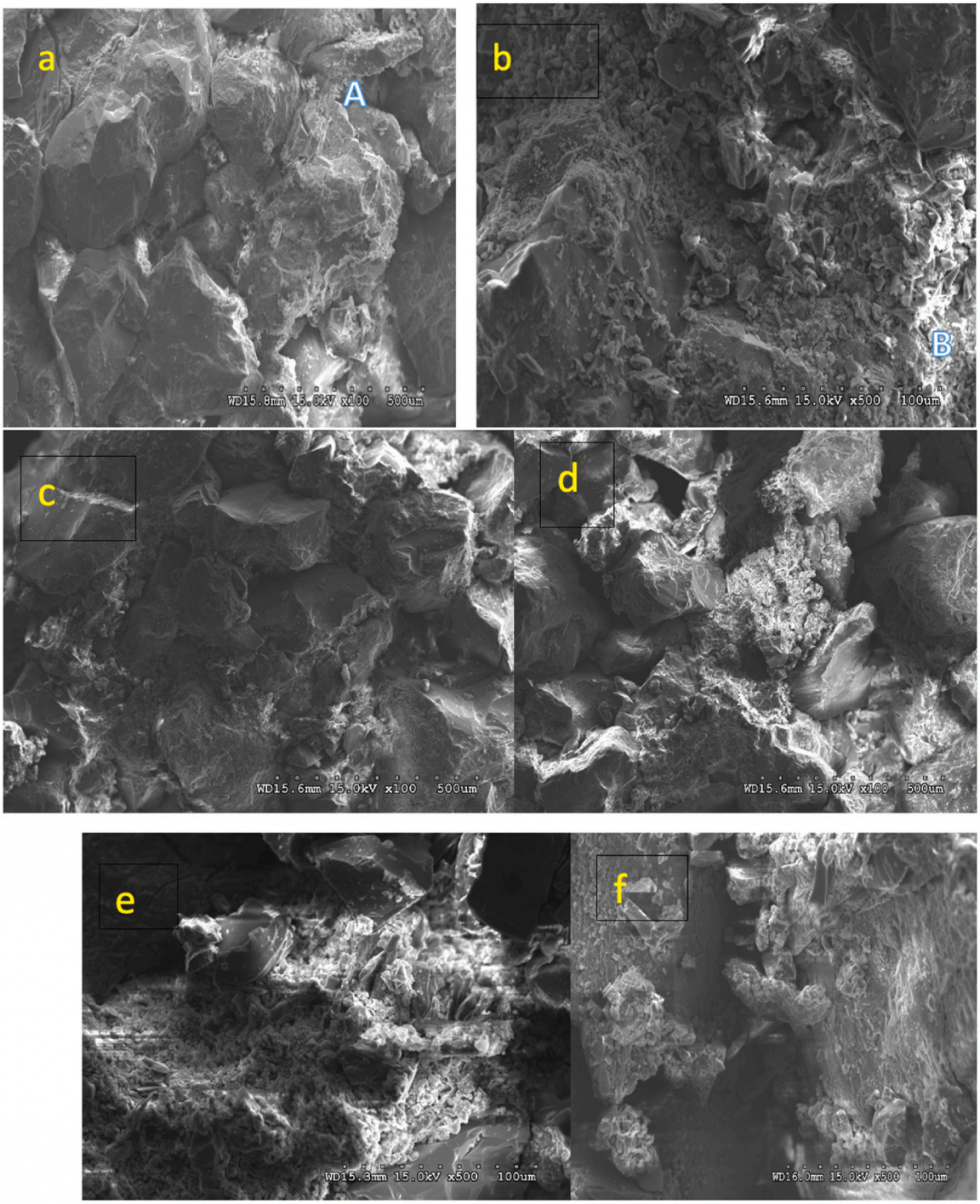

Fig. 16. SEM photomicrographs of S-4 core sample 7H at depth 10,908.50 ft showing (a) WE – face (Before), (b) WE - face (After), (c) FE-face (Before), (d) FE – face (After), (e) WE – inside (After) and (f) FE – inside (After). Sites of EDS analysis are indicated A and B.

production – Fig. 14e). However, clay minerals and pore structures in the FE – face (After back production - Fig. 14d) have been corroded, leading to an alteration in the spatial disposition of the clay minerals. A similar alteration mechanism was observed in the region of the FE – 2 mm inside (After back production – Fig. 14f). Corrosion, destabilization, and migration are commonly observed within pore walls containing kaolinite after interaction with drilling fluids (Civan, 2015; Pittman, 1989; Denniss et al., 2007; Davis and Wood, 2004). EDS analysis at location A of Fig. 14 identified high silicon and aluminium element peaks (Fig. 15) that indicated kaolinite clay when combined with SEM observations.

3.2.4.2. Physicochemical alterations at wellbore end (WE) and formation end (FE) of S-4 core sample 7H. The SEM analysis results for the physicochemical alterations observed at wellbore end (WE) and formation end (FE) of S-4 core sample 7H are presented in Fig. 16. The individual species of clay minerals have interacted with the water-based drilling fluid PAC-UL differently, leading to alteration of the pore structural network. Consequently, different formation damage mechanisms have been observed. The formation damage mechanism observed at the WE – inside may be clay swelling of smectitic components of the mixed layer (illitic + smectic) clay species (Fig. 16e). Clay swelling was neither observed nor suspected in K-3 core sample 8H (WE – inside After)

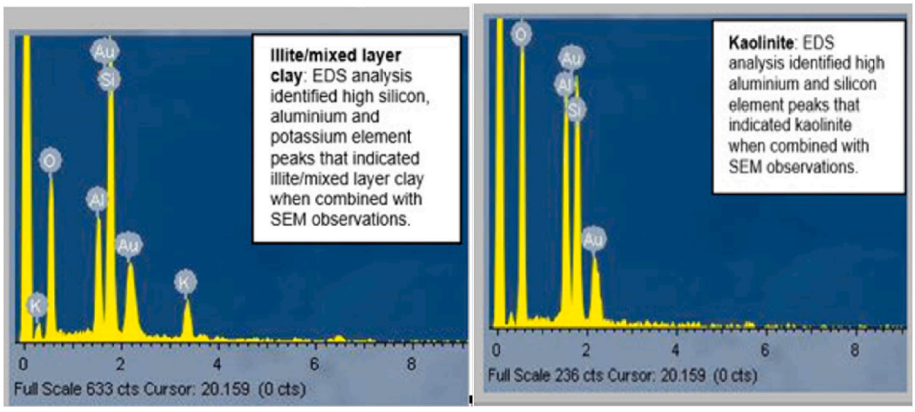

Fig. 17. EDS analysis at locations identified as A and B in Fig. 16 of sample 7H from S-4. (a) EDS at location B showing high peaks for silicon, potassium and aluminium, which is indicative of mixed-layer (illite + smectite) mineralogy and (b) EDS at location A showing high peaks for silicon and aluminium, which is indicative of kaolinite.

(Fig. 14e).

Similar to WE – face (After – Fig. 14b) and FE – face (After – Fig. 14d) in K-3 core sample 8H, corrosion and migration mechanisms were observed at the FE – face (After – Fig. 14d). Fig. 16b indicates that permeability had been severely impaired due to interaction between the base drilling fluid and the reservoir sandstone containing kaolinite and mixed layer (illite + smectite) with varying physicochemical characteristics. It has been observed and reported in another study that small pores can be damaged by swelling of mixed-layer illite/smectite clay mineralogy, while large pores suffered from the combined damage of swelling of smectite clay mineralogy and migration of hair-like illite (Zhang et al., 2020a).

EDS analysis at location B of Fig. 16 identified high silicon, aluminium, iron and potassium element peaks (Fig. 17a), indicating illite/mixed-layer clay when combined with SEM observation. On the other hand, EDS analysis at location A of Fig. 16 identified high silicon and aluminium element peaks (Fig. 17b), indicating kaolinite clay when combined with SEM observations.

3.2.5. Effects of potassium formate drilling fluid on physiochemical alteration of sandstone reservoir with varying clay mineralogy

The presence of certain clay mineralogy in the formation has shown that potassium salt inhibitory agents do not have the inhibitive effect but instead increases dispersion of clay minerals (Abass et al., 2006; Santarelli and Carminati, 1995). The inhibitory effects of potassium formate drilling fluid were tested using S-4 core sample 3H and K-3 core sample 5H in the previous section. The geometric disposition of clay minerals inside the micropore structural network was further evaluated using SEM. The results of the SEM analyses for S-4 core sample 3H and K-3 core sample 5H are presented in the following subsections.

3.2.5.1. Physicochemical alterations at wellbore end (WE) and formation end (FE) of core sample 3H S-4. The SEM analysis for the magnitude of physicochemical alterations observed at the wellbore end (WE) and formation end (FE) is presented in Fig. 18. The locations A and B in Fig. 18 represent the EDS sites identified for mixed layer (illite + smectite) at location B and kaolinite at location A, as presented in Fig. 19 (a and b).

Fines from kaolinitic and mixed layer (illite + smectite) clay mineralogy migrated or were redistributed by intra-pore migration to block the pores in the WE – face (After back production - Fig. 18b). Agglomeration of kaolinitic clay minerals and maybe swelling of smectite have been observed in the WE – inside and consequently pore structures have been plugged (After back production – Fig. 18e). The pore structures in the FE – face have been occluded by flocs of kaolinitic fines maybe vermicular and mixed layer (illite + smectite) maybe platy (After back production: Fig. 18d). On the contrary, the pore structures in FE inside (After back production) have been blocked due to migration of kaolinitic fines, maybe vermicular (Fig. 18f). The K-formate drilling fluid was able to permeate deeper into the micropore structure (Al-Yami et al., 2008).

Thus, the interaction between the K-formate drilling fluid and the kaolinite and mixed-layer (illite + smectite) clay mineralogy found in the sandstone reservoir has impaired permeability due to unfavourable electrostatic interaction between K-formate drilling fluids and clay particles. The weakening of the attractive components of the diffuse double layer electric, resulting from the detached and migrated fines that have plugged pore throats due to the shrinking of clay particles, can be attributed to the unfavourable electrostatic interaction (Zhao et al., 2018). The plugging of the main pore throats in S-4 core sample 3H and the subsequent damage after interaction with the K-formate drilling fluid can also be possibly attributed to the swelling of the mixed-layer (illite + smectite) clay mineralogy.

The severity of the formation damage depends on the presence of smectite, and if permeating K-formate drilling fluid encounters swellable clay, it depends on the size of the pore throat, which aligns with the findings of (Zhao et al., 2018). The K-formate drilling fluid was able to intercalate into the clay interlayer and replace water molecules. However, it could not effectively restrain the hydration and swelling of smectite clay materials because the hydrogen bond between water and smectite clay materials was stronger than the electrostatic interactions between K-formate drilling fluids and the clay surface. Hence, K-formate could not displace water, and the damage reaction mechanism due to ion adsorption of potassium ion (K+) most likely did not occur or on a minimal scale. This is a possible reason why EDS did not detect high peaks for K+ (Fig. 19). The SEM analysis showed a higher level of micronization after the test, decreased size number, and fewer open available pore throats compared to the water-based drilling fluid PAC-UL - S-4 core sample 7H interaction, which generated clay fines with a larger diameter and relatively more stability within the pore structures. One major reason for the poor performance of the potassium formate drilling fluid compared to the result of the water-based drilling fluid PAC-UL (Fig. 16) is the migration of fine clay particles.

3.2.5.2. Physicochemical alterations at wellbore end (WE) and formation end (FE) of K-3 core sample 5H. The result of the SEM analysis for the magnitude of physicochemical alterations observed at the wellbore end (WE) and formation end (FE) for K-3 core sample 5H are presented in

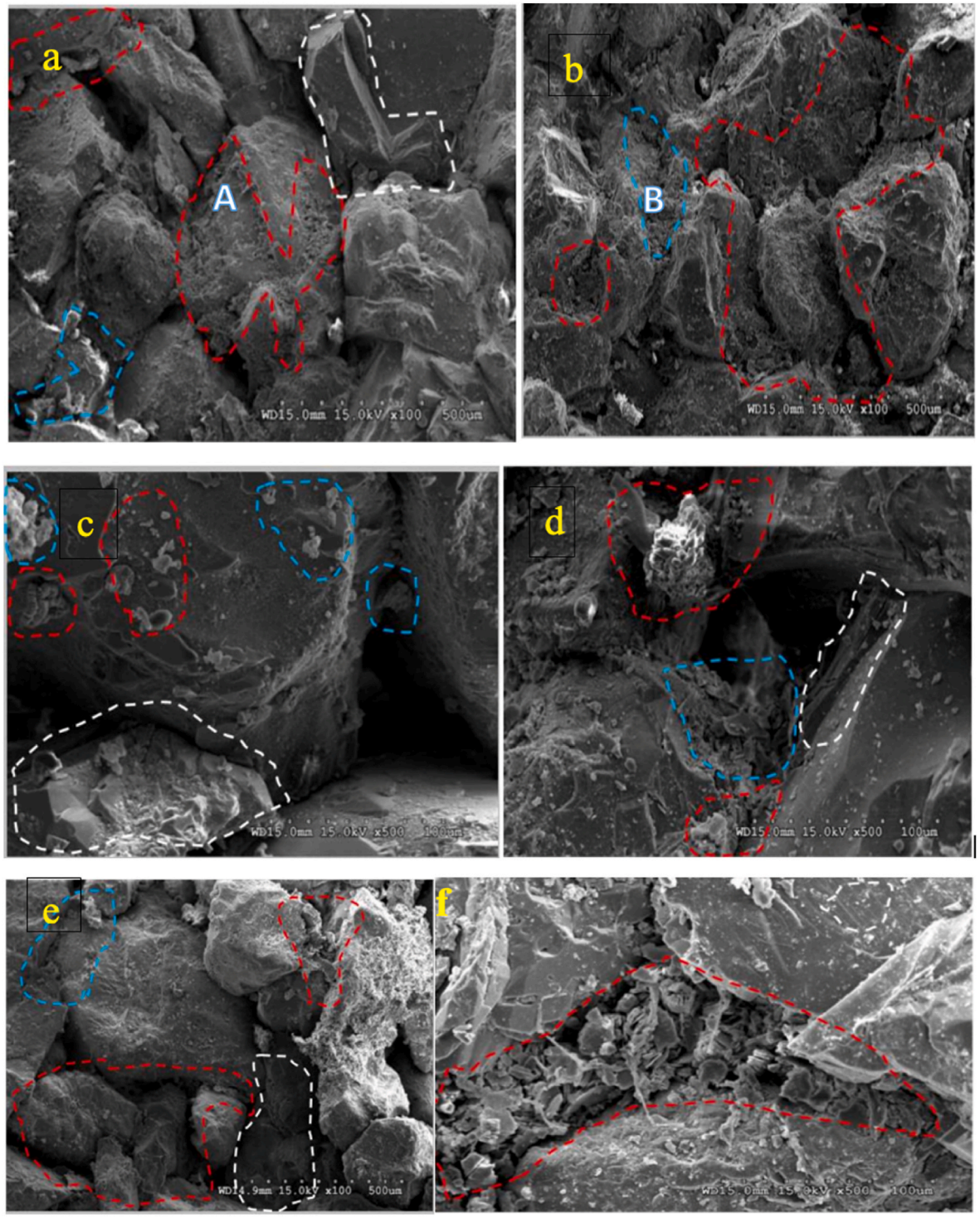

Fig. 18. SEM photomicrographs of S-4 core sample 3H at depth 10181.25 ft showing (a) WE – face (Before), (b) WE - face (After), (c) FE-face (Before), (d) FE – face (After), (e) WE – inside (After) and (f) FE – inside (After). Sites of EDS analysis are indicated A and B (red dotted lines indicating the presence of kaolinite; blue dotted lines indicating the presence of mixed layer illite + smectite; white dotted lines indicating the presence quartz growth) mineralogy.

Fig. 20. The result of the EDS analysis at sites A and B of Fig. 20 are shown in Fig. 21.

The features observed in the WE – inside (After) and FE – inside (After) for K-3 were similar to the features in WE (After) and FE (After). Therefore, no SEM photomicrograph was presented for the WE – inside (After) and FE – inside (After). The SEM photomicrographs for WE (Figures: 20a & 20 b) have revealed that the native pore-lining and pore-coating kaolinitic clay fines, with varying physicochemical properties, have detached and rearranged through intra-pore migration, leading to reduction in average return permeability as observed in Fig. 11b. The K-formate drilling fluid has caused corrosion, deflocculation, and migration (Figures: 20a & 20 b). Corrosion, destabilization and migration are commonly observed within pore walls containing kaolinite after interaction with drilling fluids (Civan, 2015; Pittman, 1989; Denniss et al., 2007; Davis and Wood, 2004).

As shown in the result presented in Fig. 20 (c & d), agglomeration

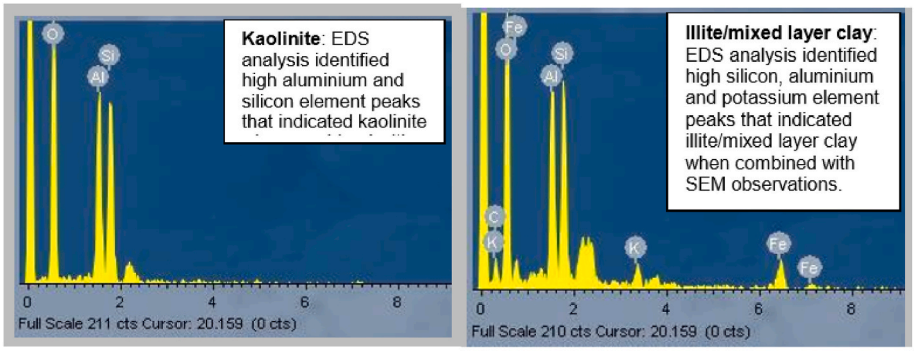

Fig. 19. EDS analysis at locations identified as A and B in Fig. 18 of sample 3H from S-4. (a) EDS at location A showing high peaks for Silicon and Aluminium, which is indicative of kaolinite and (b) EDS at location B showing high peaks for Silicon, Potassium and Aluminium, which is indicative of mixed-layer (illite + smectite) mineralogy.

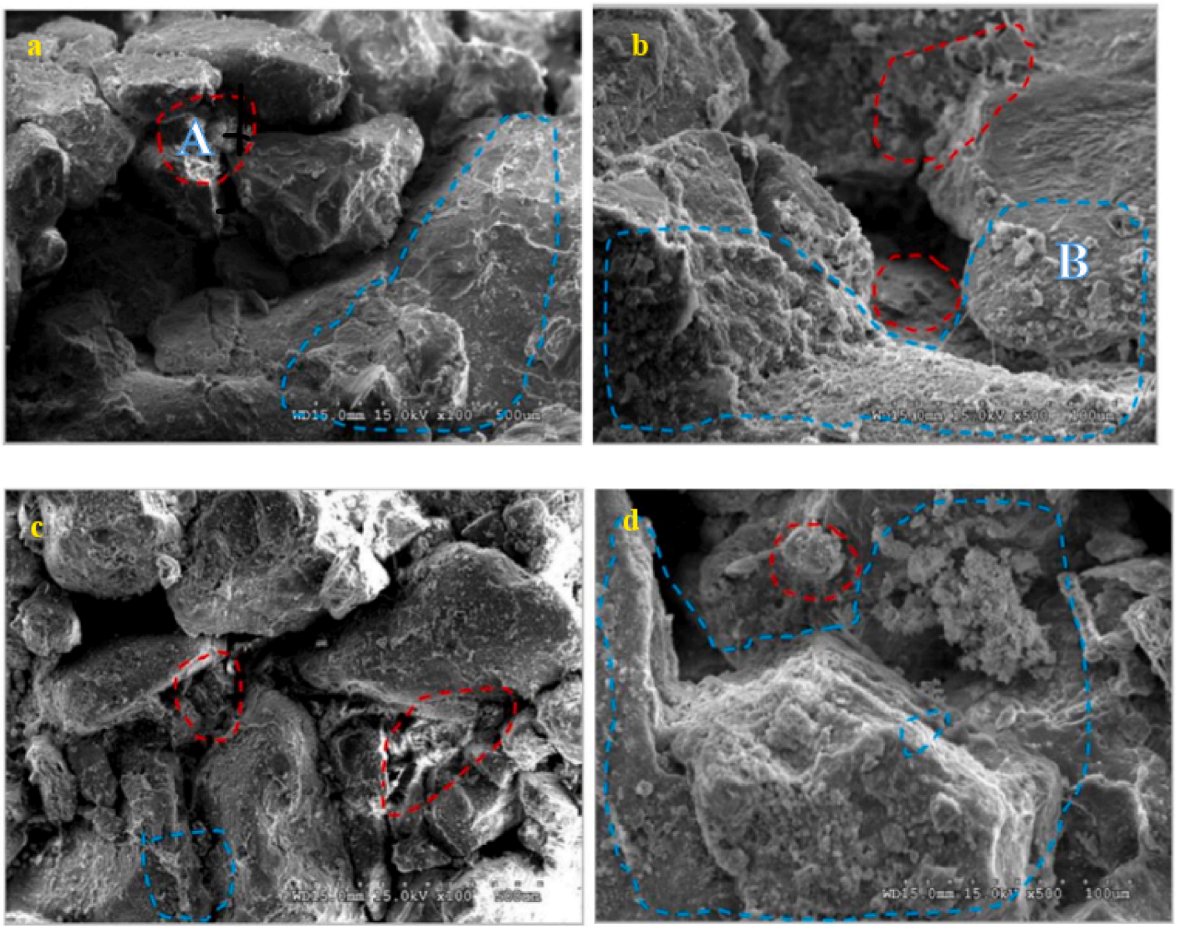

Fig. 20. SEM photomicrographs of K-3 core sample 5H at depth 7500.60 ft showing (a) WE – face (Before), (b) WE - face (After), (c) FE-face (Before) and (d) FE – face (After). Red dotted lines the presence of indicating block-like kaolinite and blue dotted lines indicating the presence of plate-like kaolinite.

and intra-pore migration occurred at the FE due to the presence of vermicular-Kaolinitic clay fines, with diameter up to 55 μm, which are larger than the smallest pore throat diameters (<1 μm). Intra pore migration can occur where the diameter of clay fines is greater than pore throat diameters (Denniss et al., 2007). The EDS analysis at location A in Fig. 20 has identified high Silicon and Aluminium element peaks (Fig. 21), indicating the presence of kaolinite clay when combined with SEM observations.

3.2.6. Effects of halide drilling fluid on physiochemical alteration of sandstone reservoir with varying clay mineralogy

The strategy used to investigate the physicochemical alterations was discussed in the preceding sections for water-based drilling fluid PAC-UL and K-formate drilling fluid respectively. The same strategy was applied to investigate the physicochemical alterations caused by the improved halide drilling fluids, which will be discussed in the following subsections.

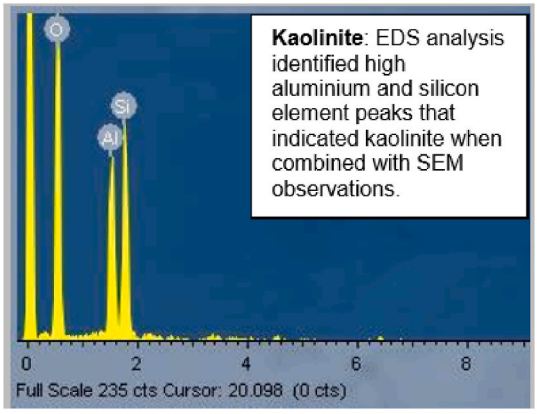

Fig. 21. EDS at location A showing high peaks for Silicon and Aluminium, which is indicative of kaolinite in K-3 core sample 5H. The EDS at location A is similar to location B.

3.2.6.1. Physicochemical alterations at wellbore end (WE) and formation end (FE) of core sample 4H S-4. The SEM analysis results for the physicochemical alterations observed at the wellbore end (WE) and formation end (FE) of S-4 core sample 4H are presented in Fig. 22. Fig. 22b shows the presence of xenomorph or anhedral, blocky pore lining and pore filling particulates from the halide drilling fluid. The result of the SEM photomicrograph (Fig. 22b) indicates that physicochemical characteristics of the micropore structure have been disrupted as result of interaction between the halide drilling fluid and the kaolinite and mixed layer (smectite + illite) clay mineralogy. Disruption of native spatial disposition of kaolinite and mixed layer (smectite + illite) clay mineralogy within the micropore structures can lead to migration through pore throat openings (Hayatdavoudi and Ghalambor, 1996; Nguyen et al., 2007; Lever and Dawe, 1984; Sharma and Yortsos, 1987), away from wellbore face. However, the stability between the micropore walls and clay fines from kaolinite and mixed layer (illite + smectite) clay mineralogy was not totally disrupted, resulting in reduced migration. This is attributed to chemical interactions between the applied halide drilling fluid phase and the native kaolinitic and mixed-layer illite + smectite, whereas increased migration was observed in the cases of formate drilling fluid and water-based drilling fluid PAC-UL. Migration of clay minerals can occur due to the interaction between drilling fluids and oil and gas reservoir rocks (Wilson et al., 2014; Mody and Hale, 1993; Khodja et al., 2010; Lal, 1999).

The result of the SEM photomicrographs for the formation end for reservoir represented by core sample 4H are shown in Fig. 22d. The SEM photomicrograph result presented in Fig. 22d indicates the presence of drilling fluid solid constituents in the formation end. EDS analysis at location A in Fig. 22 identified high Silicon, Aluminium, Iron, and Potassium element peaks, indicating the presence of illite/mixed-layer clay when combined with EDS observations (Fig. 23c). On the other hand, EDS analysis at location B of Fig. 22 identified high Silicon and Aluminium element peaks (Fig. 23b), indicating the presence of kaolinite clay when combined with SEM observations. EDS analysis at location C of Fig. 22 identified a high peak of calcium element, indicating drilling fluid constituents when combined with SEM observations

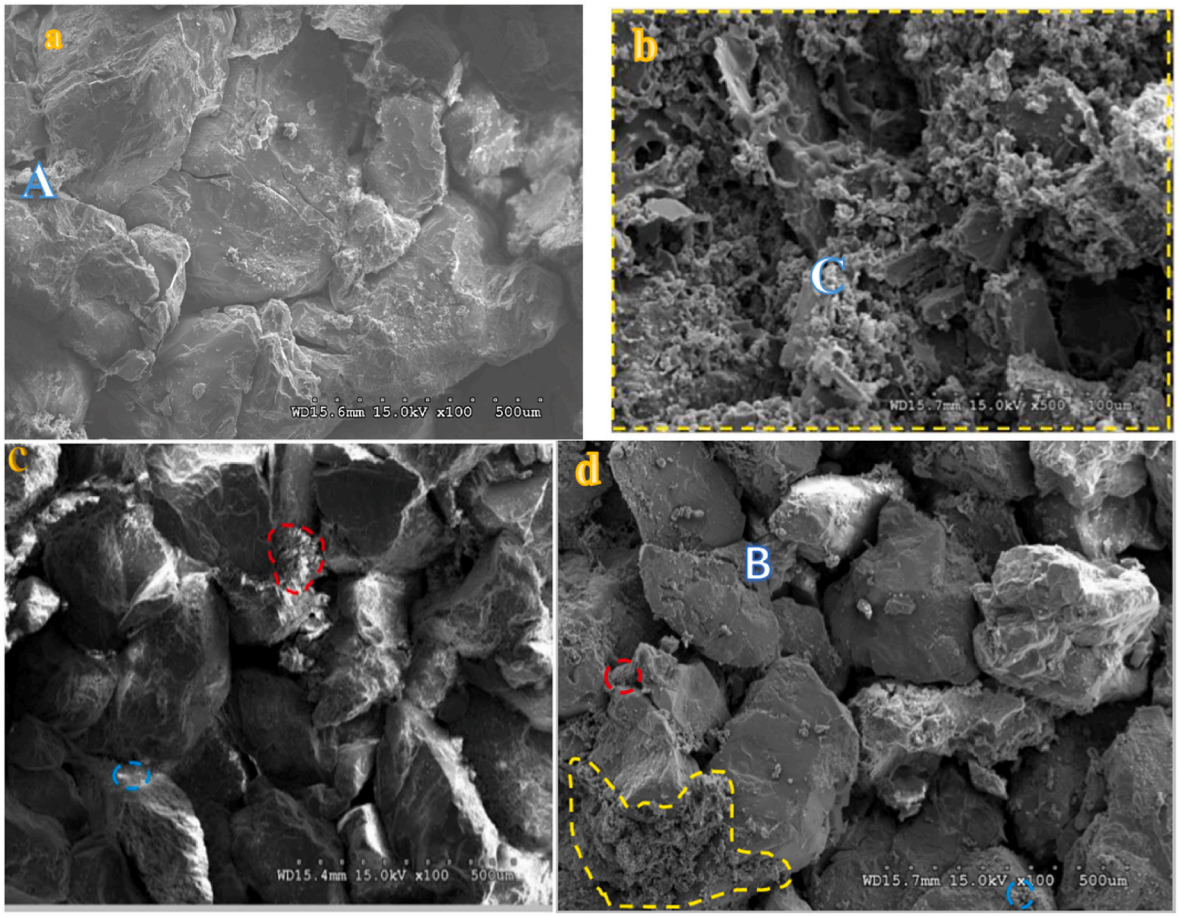

Fig. 22. SEM photomicrographs of S-4 core sample 4H at depth 10923.50 ft showing (a) WE – face (Before), (b) WE - face (After), (c) FE-face (Before) and (d) FE – face (After). Yellow dotted lines indicating the presence of drilling mud constituents; red dotted lines indicating the presence of mixed layer (illite + smectite); and blue dotted lines indicating kaolinite.

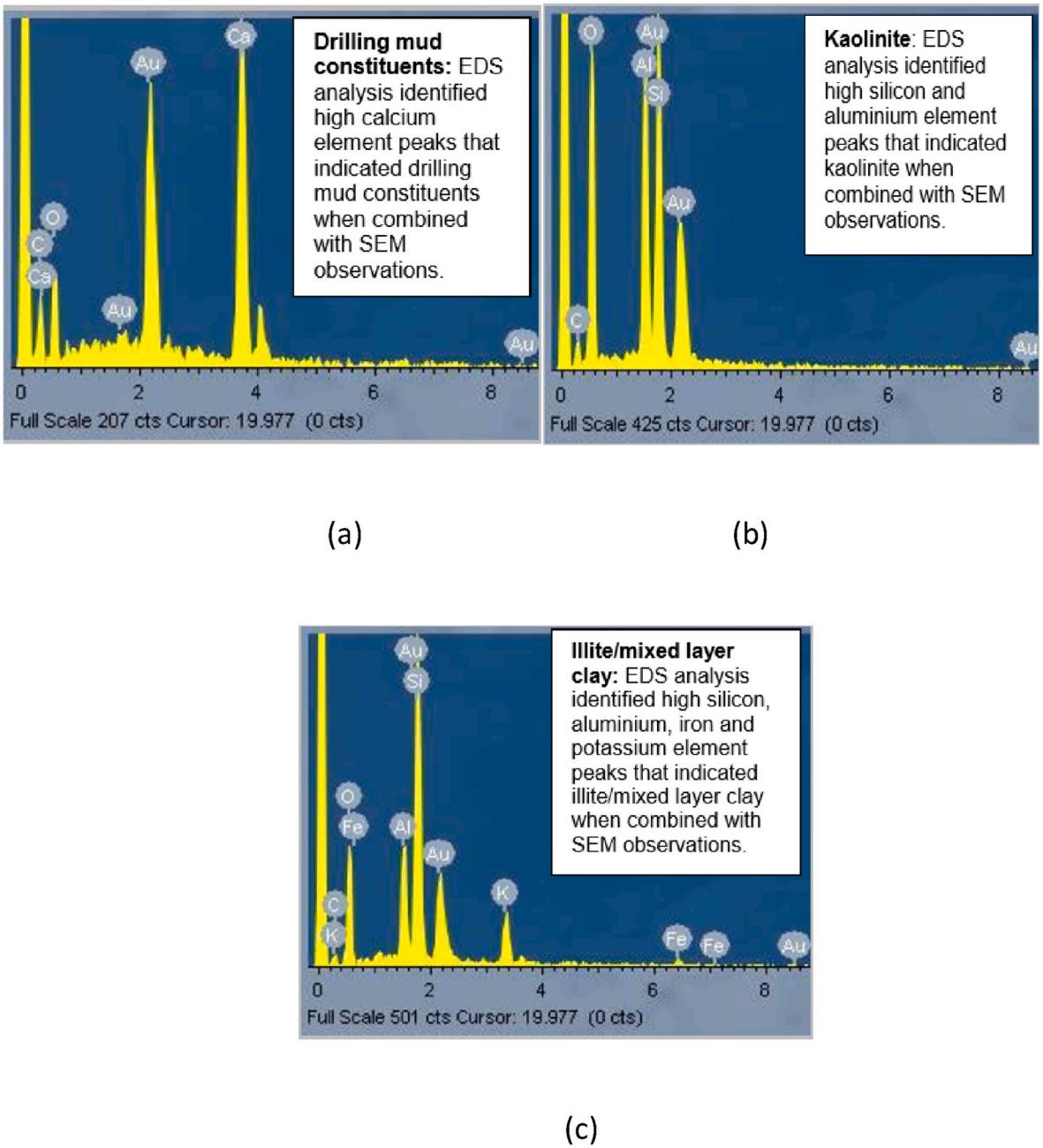

Fig. 23. EDS analysis at locations identified as A, B and C in Fig. 22 of sample 3H from S-4. (a) EDS at location C showing high peak for calcium indicative of drilling fluid (b) EDS at location A showing high peaks for Silicon and Aluminium, which is indicative of kaolinite and (c) EDS at location B showing high peaks for Silicon, Potassium and Aluminium, which is indicative of mixed-layer (illite + smectite) mineralogy.

(Fig. 23a).

3.2.6.2. Physicochemical alterations at wellbore end (WE) and formation end (FE) of K-3 core sample 6H. The results of the SEM analysis for the physicochemical alterations observed at the wellbore end (WE) and formation end (FE) after the formation damage return permeability test for halide drilling fluid on core sample 6H are presented in Fig. 24 (a, b, c, and d).

The SEM photomicrographs results presented in Figures (24a and 24b) indicate that pores have been lined and filled by an abundant amount of drilling muds constituents from the halide drilling fluid due to interaction between the kaolinite clay mineralogy and the halide drilling fluid. One critical factor in designing low-damage fluids to prevent the invasion of solids and filtrate into the production zone is sizing particles in the drilling fluid to create a surface bridge on the subterranean formation face with minimal penetration of solids and filtrate (Darley and Gray, 2011; Zhang et al., 2014). The D_{10}, D_{50}, D_{95} used in the preparation of bridging particle distribution in the halide drilling fluid formed an effective filter cake that bridged the kaolinite dominated micropore structures with pore size distribution between 1 μm and less than 50 μm (Fig. 24b), and the largest particle size that can pass through this pore is 50 μm. The filter cake can also reduce drilling fluids invasion into the drilled formation (Hossain and Al-Majed, 2015; Bourgoyne et al., 1986), as shown in Fig. 24b where the largest particle size in the halide drilling fluid was 66 μm. Therefore, achieving optimum well productivity with minimal formation damage to the reservoir and ensuring safe drilling and completion operations depend on the performance of drilling fluids (Karakosta et al., 2020). The halide drilling fluid was able to keep the

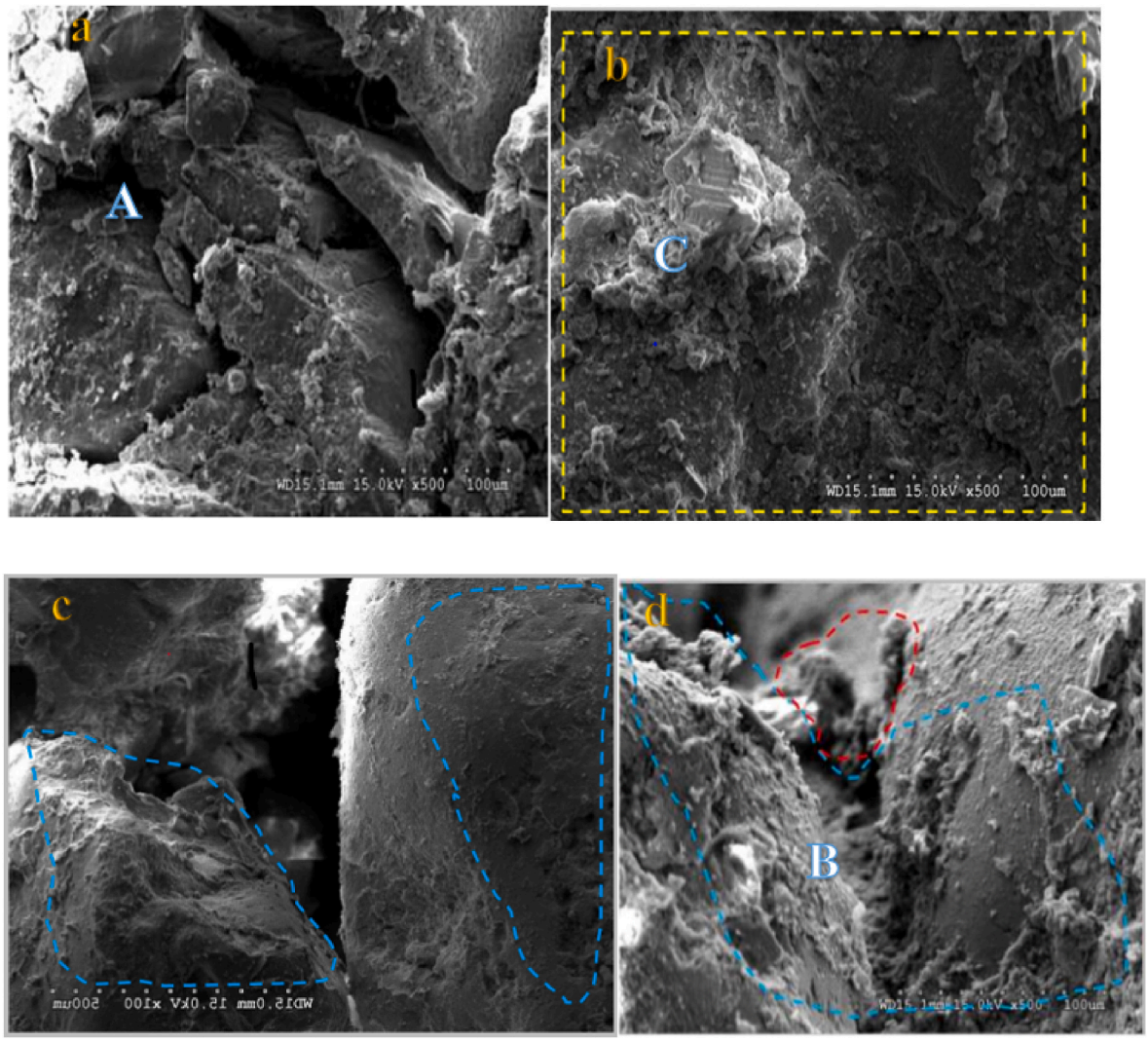

Fig. 24. SEM photomicrographs of K-3 core sample 6H at depth 7447.40 ft showing (a) WE – face (Before), (b) WE - face (After), (c) FE-face (Before) and (d) FE – face (After). Yellow dotted lines indicating the presence of drilling mud constituents; blue dotted lines indicating the presence plate-like kaolinite and red dotted lines indicating block-like kaolinite.

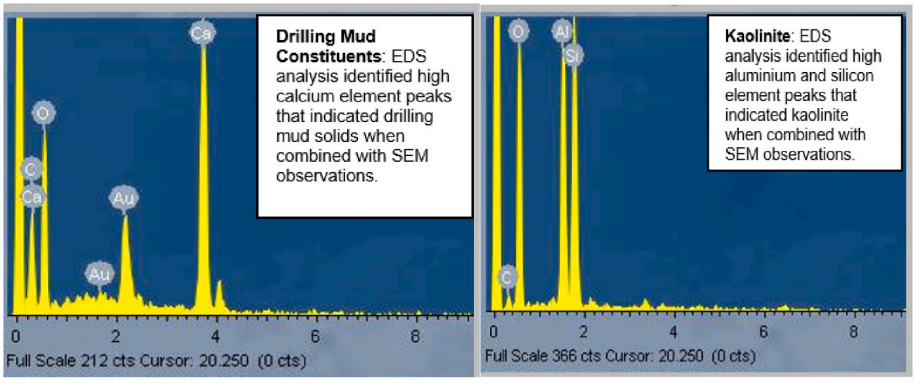

(a) (b)

Fig. 25. EDS analysis at locations identified as A and C in Fig. 24 of sample 6H from K-3. (a) EDS at location C showing high peak for calcium indicative of drilling fluid (b) EDS at locations A showing high peaks for Silicon and Aluminium, which is indicative of kaolinite. EDS at location A is similar to that of location B.

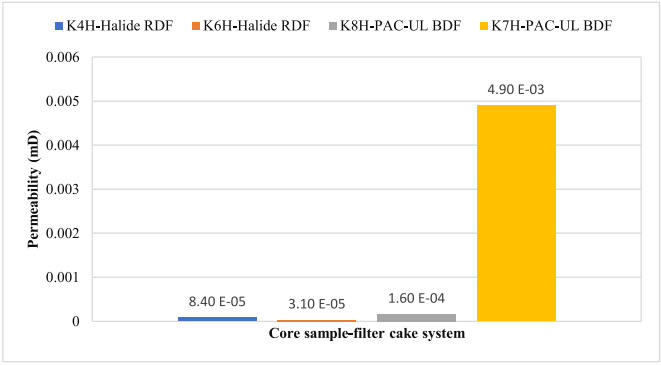

(a)

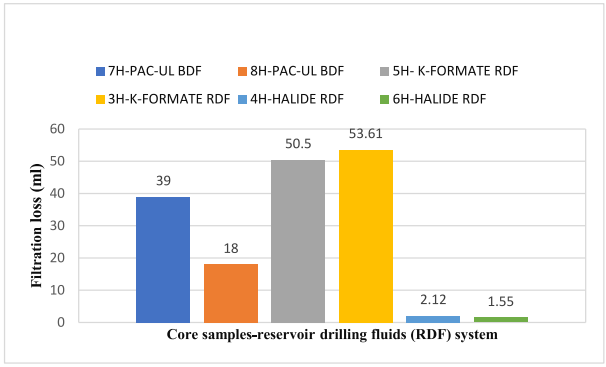

(b)

Fig. 26. Filtration behaviour of drilling fluids (a) Permeability data for k4H = 8.40 × 10–8 D, K6H = 3.10 × 10–8 D, K8H = 1.60 × 10–7 D and K7H = 4.90 × 10–6 D and (b) Filtration volumes after 60 min for base drilling fluid (BDF), halide drilling fluid and formate drilling fluids at 4,325psi and 107 °C.

kaolinitic fines in a stable state along the pore walls, reducing the level of migration (Fig. 24d), and preserving the kaolinitic fines in booklet form as pore lining without disruption or attack (Fig. 24d). This is consistent with the findings of (Al-Yami et al., 2008).

EDS analysis at location A of Fig. 24, identified high Silicon and Aluminium element peaks (Fig. 25b), indicating the presence of kaolinite clay when combined with SEM observations. The EDS analysis at location C of Fig. 24 identified high peak of calcium element, the presence of drilling fluid constituents when combined with SEM observations (Fig. 25a).

3.2.7. Effects of reservoir drilling fluid filtration behaviour on formation damage reaction mechanisms

The results of the filtration behaviour due to the interaction between RDFs of varying formulations and the core samples representing kaolinitic sandstone reservoir and mixed layer (illitic + smectitic) & kaolinitic sandstone reservoir are presented in Fig. 26a and b. The filtration test parameters were determined from experimental data during the filtration process for water-based drilling fluid PAC-UL using core samples 7H and 8H, and for halide drilling fluid using core samples 4H and 6H. The corresponding permeability values of filter cakes (K_{7H}, K_{8H}, K_{4H} and K_{6H}) were determined and are presented in Fig. 26a.

The permeability values of filter cakes $K_{7H} > K_{8H} > K_{4H} > K_{6H}$, as shown in Fig. 27a. This indicates that the filter cake of the kaolinitic reservoir-halide drilling fluid (RDF) system has demonstrated better plugging performance, fluid loss control, and minimal formation damage compared to the filter cake of the kaolinitic + mixed layer (illitic + smectitic) reservoir-halide RDF system, which has a permeability of 8.40×10^{-8} mD. The filter cakes from the base drilling fluid (BDF) and resulting systems have the highest permeability values, indicating increased formation damage.

The results of the filtration loss property are presented in Fig. 26b for the three drilling fluids (PAC-UL BDF, K-formate RDF, and halide RDF) in the kaolinitic + mixed layer (illitic + smectitic) reservoir system (represented as 7H, 3H and 4H) and kaolinitic reservoir system (represented as 8H, 5H and 6H). The best filtration loss result is observed with the halide drilling fluid and the kaolinitic reservoir system, as depicted by 6H (Fig. 26b).

In general, a filtration loss of 10 ml for the API standard filtration test at low pressure and low temperature (LPLT) conditions can be considered a low fluid loss (Færgestad and Strachan, 2014). Since HPHT conditions often result in greater fluid loss (due to lower fluid viscosity), the results obtained in this study are practically acceptable for the improved halide drilling fluid and kaolinitic reservoir system. Nevertheless, further investigation may be required to develop a better drilling fluid formulation to further reduce filtration loss in kaolinitic + mixed layer (smectitic + illitic) reservoir systems.

The detailed SEM investigation carried out in this study confirms the quantitative results of the filtration process summarized in Figures (26a and 26b). Additionally, the observations from the SEM analysis of the filter cake from the base drilling fluid with samples 7H, which has pore sizes in the range of 13 μm–20 μm, and 8H, which has pore sizes in the range of 8 μm–15 μm (Fig. 27a and b), indicate that the filter cake was very porous and permeable. This finding is corroborated by the quantitative analysis presented in Figures (27a and 27b), and as a result, increased formation damage was observed.

The SEM photomicrograph (Fig. 27c) of the filter cake for halide drilling fluid deposited on the kaolinitic reservoir represented by core sample 6H shows that it is less porous compared to the filter cake deposited on sample 8H. The filter cake in sample 6H, with pore sizes in range of 6 μm–11 μm, is less permeable compared to filter cake in sample 8H, which has pore sizes in range of 8 μm–15 μm. There was lower fluid filtration loss for the filter cake deposited on sample 6H, as confirmed by the quantitative analysis presented in Figures (26a and 26b), and minimal formation damage (Fig. 12b). A similar result was observed during analysis of the SEM photomicrograph (Fig. 27d) of the filter cake for the halide drilling fluid deposited on the kaolinitic & mixed layer (illitic + smectitic) reservoir represented by core sample 4H, which has pore sizes in the range of 13 μm–14 μm. The quantitative results are presented in Figures (26a and 26b).

In both cases, the varying clay mineralogy reacted differently with polymer and bridging materials used for the designed halide drilling fluid. However, the rare type of filter cake formed between the halide drilling fluid and core sample 6H contributed significantly to the reduced fluid loss and minimal formation damage observed (Engelhardt, 1954). The filter cake acted as a film and reduced surface area by plugging the pores. This interaction resulted in thin and less permeable filter cake with low porosities because the volume of filter cake formed per cubic centimetre of filtrate became very small (Engelhardt, 1954).

The filter cake of the halide drilling fluid deposited on the reservoir represented by core sample 6H showed little or no aggregation with the kaolinitic pore structural arrangement (Fig. 27c), hence its better hole plugging performance.

4. Conclusion

The experimental investigation indicated that the differences in performance of water-based drilling fluid PAC-UL, formate and halide drilling fluids in sandstone reservoirs containing kaolinite and mixed-layer (illite + smectite) clay mineralogy resulted from the individual differences in clay mineralogy species that have influenced the values of the return permeabilities (%), which varied between 12% and 99%. Furthermore, there are connections between the varying values of return permeability and the varying degree of micropore alterations. Therefore, all RDF can impact the microscopic alteration intensity in kaolinitic

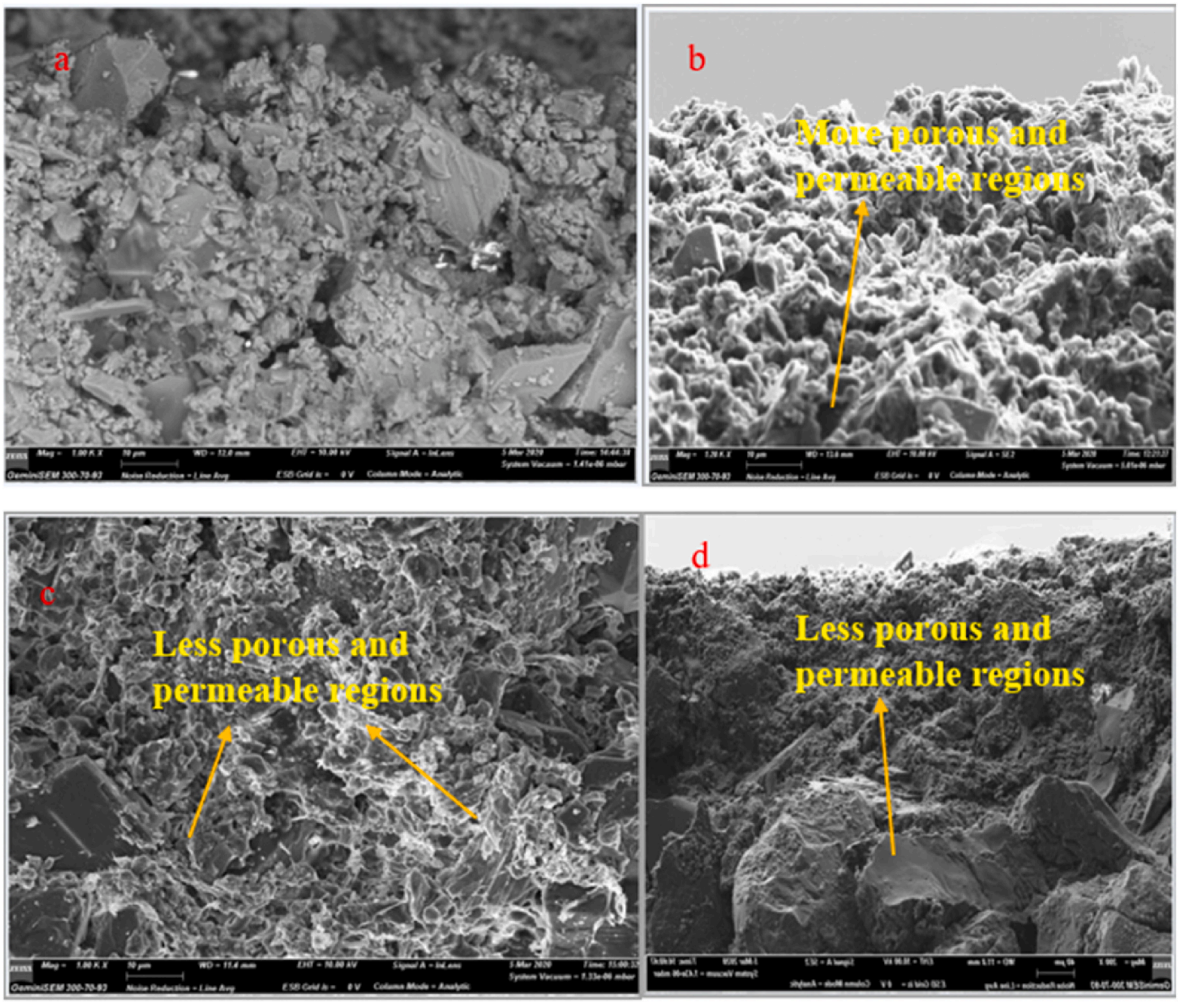

Fig. 27. SEM photomicrograph of filter cake - (a) filter cake of base drilling fluid-kaolinitic & smectitic + illitic reservoir system 7H (b) filter cake of base drilling fluid-kaolinitic reservoir system 8H (c) filter cake of halide drilling fluid-kaolinitic reservoir system-6H (d) filter cake of halide drilling fluid-kaolinitic & smectitic + illitic reservoir system 4H.

sandstone reservoirs and kaolinitic & mixed layer (smectitic + illitic) sandstone reservoirs. However, the improved halide RDF displayed better performance by lowering the microscopic alteration intensities in kaolinitic sandstone reservoirs and kaolinitic & mixed layer (smectitic + illitic) reservoirs, with the lowest microscopic alteration observed in a kaolinitic sandstone reservoir. This study confirms that existing studies have not given adequate priority to the role of individual species of clay mineralogy and their varying physicochemical properties in the development of formation damage in formulating drilling fluids for sandstone reservoir with varying clay mineralogy rather clay mineralogy is as most often the case treated as a whole or single group. Therefore, the impact of drilling fluids of varying formulations on productivity impairment of reservoir sections containing individual species of varying clay mineralogy in a micropore or mesopore structural environment has not been completely understood. The current study has provided a key reference on current practices on the principles of FDM/FDC methodology used for formulating drilling fluids specifically for kaolinitic sandstone reservoirs and therefore, the improved halide RDF is recommended for kaolinitic reservoirs.

Declaration of competing interest

The authors declare that they have no known competing financial interests or personal relationships that could have appeared to influence the work reported in this paper.

Data availability

Data will be made available on request.

Acknowledgements

Michael Chuks Halim gratefully acknowledges the financial support of Petroleum Technology Development Fund (PTDF) Nigeria through the award of PhD studentship and Seplat Petroleum Development Company for providing the core samples used for experiments.

References

Abass, H., Shebatalhamd, A., Khan, M., Al-Shobaili, Y., Ansari, A., Ali, S., Mehta, S., 2006. Wellbore instability of shale formation. In: Zuluf Field. A Paper Presented at the SPE Technical Symposium of Saudi Arabia Section,. Dhahran, Saudi Arabia. SPE-106345-MS.

Abbas, A.K., Flori, R.E., Al-Anssari, A., Alsaba, M., 2018. Testing and evaluation of shale stability for zubair shale formation. In: A Paper Presented at the SPE Kingdom of Saudi Arabia Annual Technical Symposium and Exhibition, Dammam, Saudi Arabia. P. SPE-192274-MS.

Abrams, A., 1977. Mud design to minimize rock impairment due to particle invasion. J. Petrol. Technol. 29, 586–592.

Adebayo, A.R., Bageri, B.S., 2020. A simple NMR methodology for evaluating filter cake properties and drilling fluid-induced formation damage. J. Pet. Explor. Prod. Technol. 10, 1643–1655.

Alyami, A.S., Nasr-El-Din, H.A., Al-Shafei, M.A., Bataweel, M.A., 2009. Impact of water-based drilling-in fluids on solids invasion and damage characteristics. SPE Prod. Oper. 25, 40–49.

Al-Yami, A.S., Nasr-El-Din, H.A., Bataweel, M.A., Al-Majed, A.A., Menouar, H., 2008. Formation damage induced by various waterbased fluids used to drill HP/HT wells. In: Proceedings of the SPE International Symposium and Exhibition on Formation Damage Control. Lafayette, LA, USA.
Amigun, J.O., Odole, O.A., 2013. Petrophysical properties evaluation for reservoir characterisation of Seyi oil field (Niger-Delta). Int. J. Innovat. Appl. Stud. 756–773.
Aminian, K., Bilgesu, H., Ameri, S., 1998. Influence of pore size distribution on damage profile. In: Proceedings of the SPE Formation Damage Control Conference. Lafayette, LA, USA, 18–19 February.
Bailey, L., Boek, E., Jacques, S., Boassen, T., Selle, O., Argillier, J., Longeron, D., 2000. Particulate invasion from drilling fluids. SPE J. 5, 412–419.
Bennion, D.B., 2002. An overview of formation damage mechanisms causing a reduction in the productivity and injectivity of oil and gas producing formations. J. Can. Pet. Technol. 41, 29–36.
Bin, B., Rukai, Z., Songtao, W., Wenjing, Y., Gelb, J., Gu, A., Zhang, X., Ling, S., 2013. Multi-scale method of Nano (Micro)-CT study on microscopic pore structure of tight sandstone of Yanchang Formation, Ordos Basin. Petrol. Explor. Dev. 40 (3), 354–358.
Bishop, S.R., 1997. The Experimental Investigation of Formation Damage Due to the Induced Flocculation of Clays within a Sandstone Pore Structure by a High Salinity Brine. SPE European Formation Damage Conference, The Hague, The Netherlands.
Bourgoyne, A.T., Millheim, K.K., Chenevert, M.E., Young, F.S., 1986. Applied Drilling Engineering. Society of Petroleum Engineers, Richardson, TX, USA.
Browne, S., Smith, P., 1994. Mudcake cleanup to enhance productivity of high-angle wells. In: A Paper Presented at the SPE Formation Damage Control Symposium, Lafayette. Louisiana, USA. SPE-27350-M.
Browne, S., Ryan, D., Chambers, B., Gilchrist, J., Bamforth, S., 1995. Simple approach to the cleanup of horizontal wells with prepacked screen completions. J. Petrol. Technol. 47, 794–800.
Byrne, M., 2010. Formation Damage- Any Time, Any Place, Any where. SPE Distinguished Lecturer Program. Available at: www.spe.org/dl/docs/2010/michaelByrne.pdf. (Accessed 11 December 2020).
Cabot, C., 2016. Chemical and Physical Properties Section A1 Chemistry. Available at: http://www.formatebrines.com/wp-content/uploads/2019/06/FORMATEMANUAL-A1-Chemistry.pdf. (Accessed 11 July 2019).
Civan, F., 2015. Reservoir Formation Damage. Gulf Professional Publishing: Elsevier, Boston, MA, USA.
CoÅŸkuner, G., Maini, B., 1990. Effect of net confining pressure on formation damage in unconsolidated heavy oil reservoirs. J. Pet. Sci. Eng. 4, 105–117.
Collins, N., Thaemlitz, C., 2014. Method for Drilling Using a Drilling and Completion Fluid Comprising a Phosphate Based Blend. US8901048B2.
Danilatos, G., Robinson, V., 1979. Principles of scanning electron microscopy at high specimen chamber pressures. Scanning 2, 72–82.
Darley, H.C., Gray, G.R., 2011. Composition and Properties of Drilling and Completion Fluids. Gulf Professional Publishing, Elsevier, Boston, MA, USA.
Davis, B.B., Wood, W.D., 2004. Maximizing Economic Return by Minimizing or Preventing Aqueous Phase Trapping during Completion and Stimulation Operations. A Paper presented at the SPE Annual Technical Conference and Exhibition, Houston, Texas. SPE-90170-MS.
Dejtaradon, P., Hamidi, H., Chuks, M.H., Wilkinson, D., Rafati, R., 2019. Impact of ZnO and CuO nanoparticles on the rheological and filtration properties of water-based drilling fluid. Colloids Surf. A Physicochem. Eng. Asp. 570, 354–367.
Denniss, E., Patey, I.T.M., Byrne, M.T., 2007. Cryogenic Scanning Electron Microscope Analysis: an Aid to Formation Damage Assessment, A Paper Presented at the European Formation Damage Conference, Scheveningen, The Netherlands. SPE-107560-MS.
Doane, R., Bennion, D., Thomas, F., Bietz, R., Bennion, D., 1999. Special core analysis designed to minimize formation damage associated with vertical/horizontal drilling applications. J. Can. Pet. Technol. 38. PETSOC-99-05-02.
Dong, H., Blunt, M.J., 2009. Pore-network extraction from micro-computerized-tomography images. Phys. Rev. 80, 036307.
Downs, J., 1992. Formate brines: new solutions to deep slim-hole drilling fluid design problems. In: Proceedings of the European Petroleum Conference. Cannes, France.
Engelhardt, W.V., 1954. Filter Cake Formation and Water Losses in Deep Drilling Muds. Illinois Geological Survey Library, Circular, pp. 191–194, 1954.
Epelle, E.I., Gerogiorgis, D.I., 2020. A review of technological advances and open challenges for oil and gas drilling systems engineering. AIChE J. 66, e16842.
Fang, W., Jiang, H., Li, J., Li, W., Li, J., Zhao, L., Feng, X., 2016. A new experimental methodology to investigate formation damage in clay-bearing reservoirs. J. Pet. Sci. Eng. 143, 226–234.
Færgestad, I.M., Strachan, C.R., 2014. Developing a high-performance, oil-base fluid for exploration drilling. Oilfield Rev. 26, 26–33.
Filimonova, I., Komarova, A., Provornaya, I., Dzyuba, Y., Link, A., 2020. Efficiency of oil companies in Russia in the context of energy and sustainable development. Energy Rep. 6, 498–504.
Fleming, N., Moldrheim, E., Teigland, E., Mathisen, A., 2020. Systematic approach to well productivity evaluation to determine the significance of formation damage for wells drilled in a depleted reservoir without bridging particles: oseberg main case history. SPE Prod. Oper. 35, 681–690.
Francis, P., Eigner, M., Patey, I., 1995. Visualisation of drilling-induced formation damage mechanisms using reservoir conditions core flood testing. In: A Paper Presented at SPE European Formation Damage Conference. The Hague, (Netherlands), pp. 15–16.
French, P., Mannhardt, K., De Bree, N., Shaw, J., 1995. Asessment of solvent extraction efficiency in sandstones using BET specific surface area measurements. J. Can. Pet. Technol. 34. PETSOC-95-03-03.
Gao, C.H., 2019. A survey of field experiences with formate drilling fluid. SPE Drill. Complet. 34, 450–457.
Gomez, S., Ke, M., Patel, A., 2015. Selection and application of organic clay inhibitors for completion fluids. In: A Paper Presented at the SPE International Symposium on Oilfield Chemistry. The Woodlands, Texas, USA. SPE-173731-MS.
Hayatdavoudi, A., Ghalambor, A., 1996. Controlling formation damage caused by kaolinite clay minerals: Part I. In: Proceedings of the SPE Formation Damage Control Symposium. Lafayette, LA, USA.
He, W., Stephens, M.P., 2011. Bridging particle size distribution in drilling fluid and formation damage. In: Proceedings of the *SPE* Formation Damage Conference. Noordwijk, The Netherlands.
Hillier, S., 1999. Quantitative Analysis of Clay and Other Minerals in Sandstones by X-ray Powder Diffraction (XRPD). John Wiley & Sons, Hoboken, NJ, USA.
Hossain, M.E., Al-Majed, A.A., 2015. Fundamentals of Sustainable Drilling Engineering. John Wiley & Sons, Hoboken, NJ, USA.
Howard, S.K., 1995. Formate brines for drilling and completion: state of the art. In: Proceedings of the SPE Annual Technical Conference and Exhibition. Dallas, TX, USA.
Hu, D., Wyatt, D., Chen, C., Martysevich, V., 2015. Correlating recovery efficiency to pore throat characteristics using digital rock analysis. In: A Paper Presented at the SPE Digital Energy Conference and Exhibition. The Woodlands, Texas, USA. SPE-173393-MS.
Hughes, R.V., 1950. The application of modern clay concepts to oilfield development SPE Drill. Prod. Practice 151–167.
International Energy Agency, 2020. Energy Database. https://www.iea.org/statistics/Google. (Accessed 11 December 2020).
Jev, B., Kaars-Sijpesteijn, C., Peters, M., Watts, N., Wilkie, J., 1993. Akaso field, Nigeria: use of integrated 3-D seismic, fault slicing, clay smearing, and RFT pressure data on fault trapping and dynamic leakage. AAPG Bull. 77, 1389–1404, 1993.
Jiaojiao, G., Jienian, Y., Zhiyoong, L., Zhong, H., 2010. Mechanisms and prevention of damage for formations with low-porosity and low-permeability. China. In: A Paper Presented at the International Oil and Gas Conference and Exhibition in Beijing. SPE-130961-MS.
Jin-Gang, H., Kang, Y., You, L., 2013. Damage evaluation of fracturing fluids on sandstone reservoir with extra-low permeability. Oilfield Chem. 30, e178.
Kang, Y., Luo, P., 2007. Current status and prospect of key techniques for exploration and production of tight sandstone gas reservoirs in China. Petrol. Explor. Dev. 34, 239.
Kang, Y., Xu, C., You, L., Yu, H., Zhang, B., 2014. Comprehensive evaluation of formation damage induced by working fluid loss in fractured tight gas reservoir. J. Nat. Gas Sci. Eng. 18, 353–359.
Kang, Y., Tan, Q., You, L., Zhang, X., Xu, C., Lin, C., 2019. Experimental investigation on size degradation of bridging material in drilling fluids. J. Powd. Technol. 342, 54–66.
Karakosta, K., Mitropoulos, A.C., Kyzas, G.Z., 2020. A review in nanopolymers for drilling fluids applications. J. Mol. Struct. 1227, 129702.
Khilar, K.C., Fogler, H.S., 1987. Colloidally induced fines migration in porous media. Rev. Chem. Eng. 4, 41–108.
Khilar, K.C., Vaidya, R.N., Fogler, H.S., 1990. Colloidally-induced fines release in porous media. J. Pet. Sci. Eng. 4, 213–221.
Khodja, M., Canselier, J.P., Bergaya, F., Fourar, K., Khodja, M., Cohaut, N., Benmounah, A., 2010. Shale problems and water-based drilling fluid optimisation in the Hassi Messaoud Algerian oil field. Appl. Clay Sci. 49 (4), 383–393.
Kia, S., Fogler, H.S., Reed, M., Vaidya, R., 1987. Effect of salt composition on clay release in Berea sandstones. SPE Prod. Eng. 2, 277–283.
Kibria, A., Akhundjanov, S.B., Oladi, R., 2019. Fossil fuel share in the energy mix and economic growth. Int. Rev. Econ. Finance 59, 253–264.
Klepikov, V.P., Klepikov, V.V., 2020. Quantitative approach to estimating crude oil supply in Southern Europe. Res. Pol. 69, 101787.
Krueger, R., 1967. Effect of pressure drawdown on clean-up of clay-or silt-blocked sandstone. J. Petrol. Technol. 19, 397–403.
Lal, M., 1999. Shale stability: drilling fluid interaction and shale strength. Jakarta, Indonesia. In: A Paper Presented at the SPE Asia Pacific Oil and Gas Conference and Exhibition, pp. 20–22. SPE-54356-MS.
Lever, A., Dawe, R.A., 1984. Water-sensitivity and migration of fines in the hopeman sandstone. J. Petrol. Geol. 7, 97–107.
Longeron, D., Alfenore, J., Salehi, N., Saintpère, S., 2000. Experimental approach to characterize drilling mud invasion, formation damage and cleanup efficiency in horizontal wells with openhole completions. Louisiana, USA. In: A Paper Presented at SPE International Symposium on Formation Damage Control, Lafayette. SPE-58737-MS.
Masikewich, J., Bennion, D., 1999. Fluid design to meet reservoir issues - a process. J. Can. Pet. Technol. 38, 61–71.
Mody, F.K., Hale, A.H., 1993. Borehole-stability model to couple the mechanics and chemistry of drilling-fluid/shale interactions. J. Petrol. Technol. 45 (11), 1,093-1,101.
Monaghan, P., Salathiel, R., Morgan, B., Kaiser Jr., A., 1959. Laboratory studies of formation damage in sands containing clays. Transactions of the AIME 216, 209–215.
Muskat, M., Wyckoff, R., Botset, H., Meres, M., 1937. Flow of gas-liquid mixtures through sands. Transactions of the AIME 123, 69–96.
Nguyen, P.D., Weaver, J.D., Rickman, R.D., Dusterhoft, R.G., Parker, M.A., 2007. Controlling formation fines at their sources to maintain well productivity. SPE Prod. Oper. 22, 202–215. SPE-97659-PA.
Obiora, D.N., Gbenga, D., Ogobiri, G., 2016. Reservoir characterization and formation evaluation of a "Royal onshore field". Southern Niger Delta using geophysical well log data, Journal of the Geological Society of India 87, 591–600.

Omotoso, O., McCarty, D.K., Hillier, S., Kleeberg, R., 2006. Some successful approaches to quantitative mineral analysis as revealed by the 3rd Reynolds Cup contest. Clay Clay Miner. 54, 748–760.
Pittman, E.D., 1989. Problems related to clay minerals in reservoir sandstones. AAPG Bull. A082, 237–244.
Poston, S., Berry, P., Molokwu, F., 1983. Meren Field- the geology and reservoir characteristics of a Nigerian offshore field. SPE J. 35. J Pet Technol. 1983, 35, 2095–2104: P. SPE-10344-PA.
Rui, Z., Cui, K., Wang, X., Chun, J., Li, Y., Zhang, Z., Lu, J., Chen, G., Zhou, X., Patil, S., 2018. A comprehensive investigation on performance of oil and gas development in Nigeria: technical and non-technical analyses. Energy 158, 666–680.
S Siddig, O., Mahmoud, A.A., Elkatatny, S., 2020. A review of different approaches for water-based drilling fluid filter cake removal. J. Pet. Sci. Eng. 192, 107346.
Salimi, S., Ghalambor, A., 2011. Experimental study of formation damage during underbalanced drilling in naturally fractured formations. Energies 4, 1728–1747.
Santarelli, F., Carminati, S., 1995. Do Shales Swell? A Critical Review of Available Evidence, A Paper Presented at the SPE/IADC Drilling Conference. Amsterdam, Netherlands. SPE-29421-MS.
Schwark, L., Stoddart, D., Keuser, C., Spitthoff, B., Leythaeuser, D., 1997. A novel sequential extraction system for whole core plug extraction in a solvent flow-through cell—application to extraction of residual petroleum from an intact pore-system in secondary migration studies. Org. Geochem. 26, 19–31.
Sharma, M.M., Yortsos, Y.C., 1987. Fines migration in porous media. AIChE J. 33 (10), 1654–1662.
Smith, P., Browne, S., Heinz, T., Wise, W., 1996. Drilling fluid design to prevent formation damage in high permeability quartz arenite sandstones. In: Proceedings of the SPE Annual Technical Conference and Exhibition. Denver, CO, USA, 6–9 October.
Suri, A., Sharma, M.M., 2004. Strategies for sizing particles in drilling and completion fluids. SPE J. 9, 13–23. SPE-87676-PA.
Swaco, Mi, 2008. Drilling Fluids Manual. (Accessed 12 May 2018).
Tang, Y., Yang, R., Du, Z., Zeng, F., 2015. Experimental study of formation damage caused by complete water vaporization and salt precipitation in sandstone reservoirs. Transport Porous Media 107, 205–218.
Todd, A.C., Tweedie, J., English, B., 1978. Total rock characterisation of north sea sandstones with particular reference to interstitial clays. In: A Paper Presented at the SPE European Petroleum Conference. United Kingdom, London. SPE-8118-MS.
Vickers, S., Cowie, M., Jones, T., Twynam, A.J., 2006. A new methodology that surpasses current bridging theories to efficiently seal a varied pore throat distribution as found in natural reservoir formations. Wiert. Naft. Gaz 23, 501–515.
Wilson, M., Wilson, L., Patey, I., 2014. The influence of individual clay minerals on formation damage of reservoir sandstones: a critical review with some new insights. Clay Miner. 49, 147–164.
Wuyep, E., Oluyemi, G., Yates, K., Akisanya, A.R., 2018. Geomechanical effects of oilfield chemicals on sand failure in reservoir rocks. J. Pet. Sci. Eng. 165, 347–357.
Xu, Z., Li, Z., Wang, C., Adenutsi, C.D., 2016. Experimental study on microscopic formation damage of low permeability reservoir caused by HPG fracturing fluid. J. Nat. Gas Sci. Eng. 36, 486–495.
Xu, C., You, Z., Kang, Y., You, L., 2018. Stochastic modelling of particulate suspension transport for formation damage prediction in fractured tight reservoir. Fuel 221, 476–490.
Zhang, S., Jiang, G., Qing, W., Wang, L., Guo, H., Tang, X., Bai, D., 2014. Low-damaging drilling-in fluid technology used for reservoir protection. Oil Gas Sci. Res. Proj. Inst. State Oil Co. Azerbaijan Repub. (SOCAR) 1, 24–29.
Zhang, L., Zhou, F., Pournik, M., Liang, T., Wang, J., Wang, Y., 2020a. An integrated method to evaluate formation damage resulting from water and alkali sensitivity in dongping Bedrock reservoir. SPE Reservoir Eval. Eng. 23, 187–199.
Zhang, X., You, L., Kang, Y., Zhang, C., Zhang, G., Tan, Q., 2020b. Formation damage control of saline-lacustrine fractured tight oil reservoir during well drilling. Arabian J. Geosci. (13), 1–12, 2020.
Zhao, X., Qiu, Z., Sun, B., Liu, S., Xing, X., Wang, M., 2018. Formation damage mechanisms associated with drilling and completion fluids for deepwater reservoirs. J. Pet. Sci. Eng. 173, 112–121.
Zhou, C.H., Keeling, J., 2013. Fundamental and applied research on clay minerals: from climate and environment to nanotechnology. Appl. Clay Sci. 74, 3–9.